CHAPTER 5

# Parvoviral Host Range and Cell Entry Mechanisms

**Susan F. Cotmore*** and **Peter Tattersall*,†**

Contents



* Department of Laboratory Medicine, Yale University Medical School, New Haven, Connecticut 06510
† Department of Genetics, Yale University Medical School, New Haven, Connecticut 06510

Advances in Virus Research, Volume 70
ISSN 0065-3527, DOI: 10.1016/S0065-3527(07)70005-2

**Abstract**

Parvoviruses elaborate rugged nonenveloped icosahedral capsids of ~260 Å in diameter that comprise just 60 copies of a common core structural polypeptide. While serving as exceptionally durable shells, capable of protecting the single-stranded DNA genome from environmental extremes, the capsid also undergoes sequential conformational changes that allow it to translocate the genome from its initial host cell nucleus all the way into the nucleus of its subsequent host. Lacking a duplex transcription template, the virus must then wait for its host to enter S-phase before it can initiate transcription and usurp the cell's synthetic pathways. Here we review cell entry mechanisms used by parvoviruses. We explore two apparently distinct modes of host cell specificity, first that used by Minute virus of mice, where subtle glycan-specific interactions between host receptors and residues surrounding twofold symmetry axes on the virion surface mediate differentiated cell type target specificity, while the second involves novel protein interactions with the canine transferrin receptor that allow a mutant of the feline leukopenia serotype, Canine parvovirus, to bind to and infect dog cells. We then discuss conformational shifts in the virion that accompany cell entry, causing exposure of a capsid-tethered phospholipase A2 enzymatic core that acts as an endosomolytic agent to mediate virion translocation across the lipid bilayer into the cell cytoplasm. Finally, we discuss virion delivery into the nucleus, and consider the nature of transcriptionally silent DNA species that, escaping detection by the cell, might allow unhampered progress into S-phase and hence unleash the parvoviral Trojan horse.

## I. INTRODUCTION TO THE VIRUSES

### A. The family Parvoviridae

All small nonenveloped viruses with ~5-kb linear, self-priming, single-stranded DNA genomes are grouped in the taxonomic family Parvoviridae (from *Parvus*—Latin for ''small''), and share a common evolutionary history as assessed by DNA sequence. This broad group is divided into two subfamilies, superficially on the basis of host range: the Parvovirinae, infecting vertebrate hosts and the Densovirinae, infecting insects and other arthropods. While species and genera within the Parvovirinae appear to be derived from a single common ancestor, the arthropod genera are separated by massive evolutionary distances, probably reflecting divergence coincident with that of their hosts (Tattersall *et al.*, 2005). Thus,

this is an ancient and widely dispersed virus family with, apparently, a single evolutionary branch that became adapted to vertebrate hosts.

Members of the subfamily Parvovirinae have been divided into five genera on the basis of DNA and protein sequence-based phylogenetic analyses: these are the *Parvoviruses*, which are the subject of this chapter, and the *Amdoviruses*, *Bocaviruses*, *Dependoviruses*, and *Erythroviruses*. While all genera contain viruses that can replicate independently of helper viruses (commonly described as ''autonomously replicating'' viruses), the *Dependovirus* genus is so called because it includes a large number of agents that depend for their own productive replication on coinfection with a more complex helper virus from a different taxonomic family. This association with adenoviruses is reflected in the name, ''adeno-associated viruses'' (AAVs), although these same viruses may also derive help from herpesviruses, papillomaviruses, or vaccinia viruses. In the absence of such help, AAVs establish a latent interaction with their vertebrate host, and this nondisruptive, but persistent, lifestyle has engendered significant interest in them as gene therapy transfer vectors. Accordingly, they have been the focus of much recent research, so that emerging data from viruses in this genus does much to complement our current knowledge of entry processes used by their *Parvovirus* cousins, and is cited accordingly in this chapter.

The biology of the Parvovirinae is dominated by their small physical size. With nonenveloped protein capsids of around 260 Å diameter, constructed in the simplest icosahedral form ($T = 1$), these remarkably dense and rugged particles deliver their enclosed genomes into the cell, traverse the cytoplasm, and penetrate the nucleus while still comprising a structurally intact, albeit somewhat rearranged, capsid (Farr *et al.*, 2006; Sonntag *et al.*, 2006; Vihinen-Ranta *et al.*, 2002). Encapsidation within such a small virion is possible because parvoviruses typically encode just two gene cassettes, and are unique among known microorganisms in having DNA genomes that are both single stranded and linear, which makes their chromosome optimally small and flexible. This single DNA strand is inserted vectorially into a preformed capsid, using energy provided by a viral helicase, and packed in such a way that bases in the outer DNA shell bond with side chains from amino acids lining the icosahedral threefold axis of the capsid, creating a virion of remarkable density and stability (Agbandje-McKenna and Chapman, 2006; Chapman and Agbandje-McKenna, 2006). Inevitably, such minimalism has some apparently negative biological consequences. Parvoviruses not only lack accessory proteins that might induce resting cells to enter S-phase, they also lack a duplex transcription template so that they are generally unable to express their genes until the DNA synthetic machinery of the host cell, activated at the start of a cell-directed S-phase, coincidentally provides them with a complementary-sense DNA strand. Consequently,

these viruses have had to become masters of stealth, apparently avoiding triggering many of the cellular responses that commonly accompany cell entry by viruses of other families. As a result, although relatively inert, they are able to become sequestered within resting cells without inhibiting the cell's program of transit through the cell cycle. Indeed, this suggests an entry strategy in which the disadvantages of being single stranded are outweighed by the ability to package a relatively complex genome in a particle small enough to be imported intact into the host cell's nucleus.

## B. The genus *Parvovirus*

Much of our knowledge of the molecular biology and pathogenic potential of the family Parvoviridae has been derived by studying members of the genus *Parvovirus*, which typically grow efficiently in cell culture, are open to reverse and forward genetic analysis, and predominantly infect host species that are readily susceptible to experimental manipulation. This genus contains four distinct subgroups: (1) a broadly related, but serologically diverse cluster of ''rodent virus'' species that contains three distinct clades [Minute virus of mice (MVM), the type species of the genus, Mouse parvovirus 1 (MPV1), and a rat virus group that includes Rat minute virus 1 (RMV1), H1 virus and Kilham rat virus (KRV)], and LuIII, an ''orphan'' virus; (2) an outlying Rat parvovirus 1 (RPV1) branch; (3) the Feline panleukopenia virus/Canine parvovirus (FPV/CPV) serotype, strains of which infect various members of the *Carnivora*; and (4) Porcine parvovirus (PPV). As seen in Table I, the NS1 genes of species within this genus vary by up to 30%, whereas their VP2 genes vary by up to 50%, this wider range reflecting the fact that the members of each species represent a serologically distinct group. In contrast to these broad interspecies values, the intraspecies homologies for the NS1 and VP2 proteins specified by the prototype MVM strain, MVMp, and those of the ''immunosuppressive'' strain, MVMi, are both 97.8%, and for the NS1 and VP2 proteins of FPV and CPV are 99.0% and 98.6%, respectively.

Patterns of parvovirus-induced disease are largely determined by the fact that these viruses cannot induce resting cells to enter S-phase, and hence only replicate productively in actively mitotic host cell populations. They also commonly exhibit finely tuned tissue specificity, only infecting cells of particular differentiated phenotypes, although such preferences can vary profoundly even within virus strains of a single serotype. Accordingly, pathogenic or lethal infections typically occur in fetal or neonatal hosts, which have many dividing cell populations, or involve adult tissues that remain actively dividing in later life such as cells of the gut epithelium or leukocyte lineages. Acute clinical infections are typically resolved rapidly by development of a predominantly humoral

**TABLE I** Comparison of NS1 and VP2 protein sequences within the genus *Parvovirus*

| | MVM | MPV1 | KRV | RMV1 | H1 | LuIII | RPV1 | FPV | PPV | |
|---|---|---|---|---|---|---|---|---|---|---|
| MVM | 100 | 97.5 | 91.8 | 91.5 | 91.4 | 89.6 | 81.4 | 71.9 | 67.7 | MVM |
| MPV1 | 71.2 | 100 | 91.5 | 91.2 | 91.2 | 90.3 | 81.4 | 72.1 | 68.0 | MPV1 |
| KRV | 68.0 | 66.2 | 100 | 99.3 | 98.1 | 88.0 | 81.9 | 72.0 | 68.1 | KRV |
| RMV1 | 69.3 | 71.9 | 73.2 | 100 | 97.9 | 87.8 | 81.9 | 72.1 | 68.3 | RMV1 |
| H1 | 63.1 | 61.7 | 72.3 | 67.7 | 100 | 88.0 | 82.2 | 71.7 | 67.7 | H1 |
| LuIII | 71.2 | 83.5 | 66.3 | 71.9 | 64.5 | 100 | 79.2 | 70.8 | 67.5 | LuIII |
| RPV1 | 58.0 | 58.6 | 60.5 | 60.3 | 57.2 | 59.1 | 100 | 77.9 | 70.2 | RPV1 |
| FPV | 48.6 | 49.0 | 50.5 | 48.9 | 47.3 | 47.0 | 48.2 | 100 | 64.5 | FPV |
| PPV | 48.1 | 47.1 | 49.5 | 49.5 | 48.1 | 49.2 | 48.8 | 56.0 | 100 | PPV |
| | MVM | MPV1 | KRV | RMV1 | H1 | LuIII | RPV1 | FPV | PPV | |

Percent homology was calculated for each pairwise combination of NS1 (shaded) or VP2 (unshaded) polypeptides, using the Diagonals method (BLOSUM62 alignment score matrix) in DNA Strider 1.4, using a block length of 6 amino acids. Mismatch and gap penalties were set to 1 and 2, respectively.
Protein sequences were derived for a representative of each virus species, using DNA sequences data from the GenBank database, as follows: MVM, Minute virus of mice (prototype strain) [J02275]; MPV1, Mouse parvovirus 1 [U12469]; KRV, Kilham rat virus [AF321230]; RMV1, Rat minute virus 1 [AF332882]; H1, H-1 virus [X01457]; LuIII, LuIII virus [M81888]; RPV1, Rat parvovirus 1 [AF036710]; FPV, Feline panleukopenia virus [M38246]; and PPV, Porcine parvovirus (NADL-2 strain) [L23427]. Double-lined box denotes the closely related ''rodent'' subgroup described in the text.

immune response, but latency often ensues. In their natural host some viruses, most notably members of the rodent groups, are clinically silent, and can establish persistent infections associated with prolonged virus release from reservoirs that are currently unknown.

## II. STRUCTURE OF A UNIQUELY DENSE AND COMPACT VIRION

Infectious parvoviral virions are nonenveloped, ~260 Å in diameter, and contain a single-stranded, linear DNA genome of ~5 kb. They comprise between 70% and 80% protein, with the remainder being DNA, and are uniquely dense and compact, with molecular masses in the order of $5.5–6.2 \times 10^6$, sedimentation coefficients of 110S–122S, and buoyant densities of 1.39–1.43 g/cm$^3$ in cesium chloride. Mature virions are stable in the presence of lipid solvents or on exposure to pH 3–9. They are historically reported to survive prolonged incubation at 56 °C, although this characteristic applies only to concentrated suspensions of particles or in situations where they are protected by animal tissue, since in dilute solution they are metastable, undergoing an inactivating conformational transition in response to heat or denaturants. However, under natural conditions, infectious virions are exceptionally durable, surviving for weeks or months at room temperature or for several years at 4 °C.

### A. Rugged 260 Å protein capsids with T = 1 icosahedral symmetry

Parvovirus-infected cells typically generate thousands of copies of both empty capsids and full virions, with almost indistinguishable core X-ray structures. These capsids are constructed from 60 copies of a single polypeptide sequence, and hence exhibit $T = 1$ icosahedral symmetry. Virions generally contain proteins of two or three size classes (VP1–VP3) that constitute a nested set. These share a common C-terminal core sequence but have N-terminal extensions of different lengths. The largest capsid polypeptide, designated VP1, has a molecular mass of ~83,000 and is present at ~10 copies per capsid. It is dispensable for particle assembly, DNA packaging, and virion release, but is essential for infectivity (Tullis *et al.*, 1993), since it carries a series of elements that are required for trafficking through host cell entry pathways. These include a unique phospholipase domain that is deployed to breach the lipid bilayer of an endosomal vesicle. Three-dimensional structures of several wild-type and mutant parvovirus particles have been determined to near-atomic resolution by X-ray crystallography, including forms of CPV, FPV, two strains of MVM, and recombinant virus-like particles (VLPs) of PPV

(reviewed in Chapman and Agbandje-McKenna, 2006). Core structure is based on a classic eight-stranded antiparallel β-barrel, but in parvoviruses these β-strands are connected by elaborate and highly variable loops, which make up most of the viral surface (Chapman and Rossmann, 1993). The N-terminal peptide domains of the larger proteins are submolar and disordered, so their disposition cannot be deduced from X-ray data.

The outer architecture of the parvovirus capsid has a number of structural features, illustrated in Fig. 1. Each asymmetric unit has two ''spike''-like elevations, which surround the 20 threefold symmetry axes of the icosahedron, a deep depression, called the ''dimple,'' at each twofold axis, and a hollow cylinder, surrounding each of the 12 icosahedral fivefold axes, which contains a central pore that connects the inside of the virion with the particle exterior. In full virions, each pore contains a single copy of a glycine-rich sequence from a single VP2 molecule, positioned so that the N-terminal 25 amino acids of the peptide are externalized (Agbandje-McKenna *et al.*, 1998; Tsao *et al.*, 1991). These cylindrical

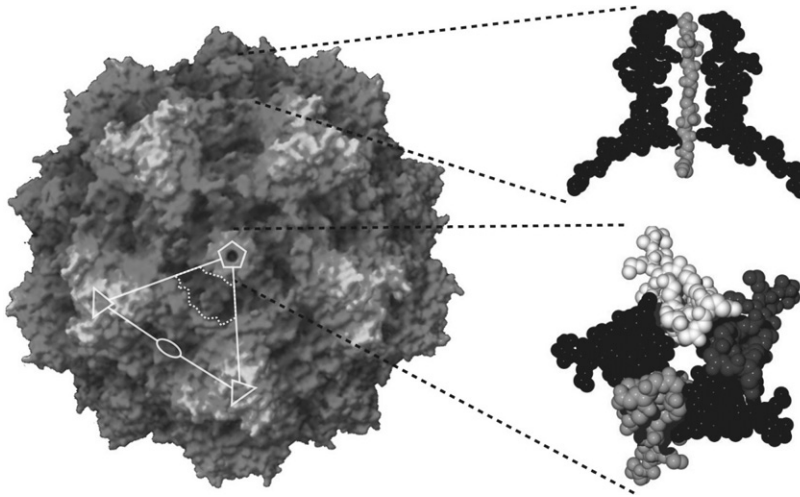

**FIGURE 1** Topology of the parvoviral particle. Left—depth-cued, space-filling model of MVM, centered on a fivefold symmetry axis (pentangle). One crystallographic asymmetric unit is indicated by the large triangle, bordered by a fivefold axis, two threefold axes (triangles), and a twofold axis (oval). Topological features seen here that are referred to in the text include the fivefold cylinder surrounded by the canyon (enclosed in dotted line), the threefold spikes and the dimple surrounding the twofold axis. Upper right—cross-section of the fivefold channel, showing two of the five β-ribbons that comprise the cylinder, and residues 28–37 of VP2 in gray. Lower right—view down the fivefold cylinder, with the five β-ribbons differentially shaded.

structures are themselves encircled on the outer virion surface by a deep, canyon-like depression with highly conserved amino acid sequence, but unknown function. Neutralizing antibody binding sites generally map to the threefold spike or to its shoulders, as do protein receptor contacts for those serotypes in which such interactions have been identified. Sequences that determine viral tissue specificity and oligosaccharide recognition lie in the twofold dimple and up the adjacent edge of the threefold spike.

## B. Linear single-stranded DNA genomes with palindromic telomeres

Mature virions of most species in this genus contain a single 5-kb DNA strand that is negative sense with respect to transcription, while one virus, LuIII, packages approximately equimolar positive- and negative-sense strands. This remarkable variability illuminates the whole process of strand selectivity, since it is caused by differential rates of initiation from the two viral replication origins rather than by any strand-specific packaging signal or mechanism (Cotmore and Tattersall, 2005b). Since most, but not all, genomes are negative sense with regard to transcription, a unifying convention has been adopted whereby the 3′ terminus of the negative strand is rather called ''the left'' end and the 5′ terminus of this strand ''the right'' end. Within the virions, some of the single-stranded DNA displays icosahedral symmetry, so that about a third of the genome can be visualized by crystallography, abutting the particle shell. This DNA has some limited nucleotide specificity, and is oriented with its bases pointing outward, forming a number of conserved protein–base hydrogen bonds with the inner surface of the capsid (Agbandje-McKenna *et al*., 1998; Xie and Chapman, 1996). Remarkably, not all of the genome is contained within the particle. DNA packaging proceeds in a 3′-to-5′ direction, but the 5′ end of the strand is left projecting through the capsid wall at an unknown location so that ~24 nucleotides (nts), called the ''tether'' sequence, are left outside the particle, covalently attached, at its 5′ end, to a single molecule of the viral replication initiator protein, NS1 (Cotmore and Tattersall, 1989).

At both termini of the linear, nonpermuted genome there are essential palindromic sequences that can fold into self-priming duplex ''hairpin'' telomeres, as illustrated at the top of Fig. 2, which are diagnostic features of this virus family. These provide most of the *cis*-acting information needed for both viral DNA replication and encapsidation. In viruses from the genus *Parvovirus*, these two terminal hairpins differ from one another in both sequence and predicted secondary structure. This disparity allows differential initiation and encapsidation of the two strands, and typically means that infected cells only receive negative-sense DNA.

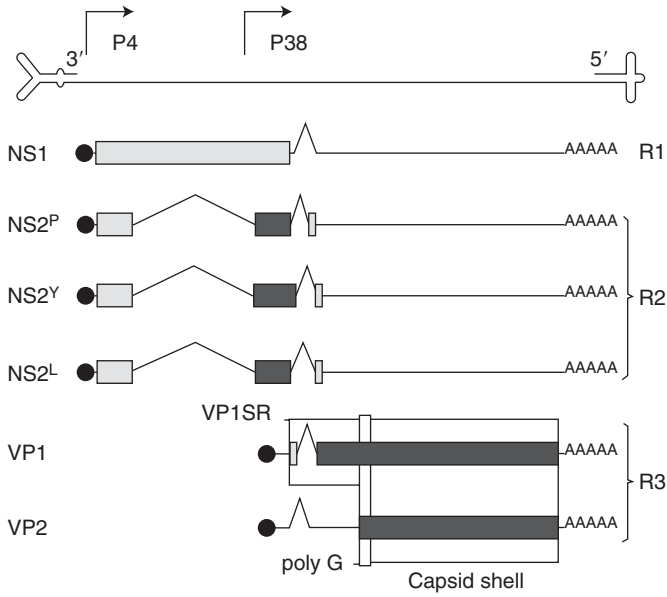


**FIGURE 2** Genetic strategy of the prototypic *Parvovirus* MVM. The single-stranded, negative-sense DNA genome is shown as a continuous line, which terminates in folded hairpin structures that are expanded ~20-fold in scale with respect to the coding sequence between them. The two viral promoters, at 4 and 38 map units, are shown by rightward arrows, and the mature, cytoplasmic transcript classes driven by each, R1, R2, and R3, are displayed below, with a black sphere indicating the capped 5′ ends and AAAA denoting their polyadenylated tails. Open reading frames (ORFs) shades specifying the viral gene products, named on the left, are displayed in different shades according to their reading phase, and their spliced-out introns are represented by the thin-lined carets. The boxes denote, from the left, the VP1-specific region involved in entry functions, the glycine rich "spacer" that occupies the fivefold pore, and the common region of the VP polypeptides, 60 copies of which comprise the $T = 1$ protein shell of the capsid.

This, in turn, may dictate the mechanism(s) of latency adopted by the virus. In contrast, members of the *Dependovirus* and *Erythrovirus* genera have inverted terminal repeat (ITR) sequences, and encapsidate strands of both senses with equal efficiency. In the genus *Parvovirus* the left-end telomere usually comprises ~120 nts and can be folded in a Y-shaped configuration, while the right-end palindrome is ~250 nts in length and is predicted to be able to alternate, with little change in free energy, between linear and cruciform configurations. These termini serve as hinges, allowing the ancient single-strand displacement ''rolling circle replication'' strategy, to be adapted for the replication of a linear genome. Protein motifs characteristic of initiator nucleases derived from these ancestral

replicons are conserved in the viral genome, and its modified replication scheme is termed ''rolling hairpin replication.''

## C. Creating and expressing transcription templates

When the cell enters S-phase, the viral 3′ hairpin acts as a primer for complementary-strand DNA synthesis, generating a duplex unit-length replicative intermediate that can support viral transcription. This contains two mRNA transcription units, with promoters at map units 4 and 38 and a single functional polyadenylation site at the extreme right-hand end (reviewed in Qiu *et al.*, 2006). These two promoters, P4 and P38, drive expression of a nonstructural gene (NS), encoded in the left half of the genome, and a capsid gene (VP), encoded in the right half, respectively. Alternative splicing events orchestrate gene expression, as shown for MVM in Fig. 2 (Cotmore and Tattersall, 1990; Jongeneel *et al.*, 1986; Morgan and Ward, 1986; Pintel *et al.*, 1983). The R1 transcripts, synthesized from the P4 promoter, contain a single contiguous open reading frame (ORF) that encodes the 83-kDa multifunctional replication initiator protein, NS1, located upstream of a complex alternately spliced small intron region. In a further set of P4-derived transcripts, R2, the NS1 ORF is spliced into an alternate reading frame by removal of the major intron, and these transcripts encode, in order of abundance, NS2P, NS2Y, and NS2L, the extreme C-termini of which are different due to the use of two pairs of alternative 5′ and 3′ splice sites bordering the small intron. In contrast, members of the FPV serotype express a single, shorter NS2 species, whose second exon is encoded in, and terminates within, the alternative reading frame, some 15 codons upstream of the small intron (Wang *et al.*, 1998).

One function of NS1 is to upregulate the P4 promoter itself, and this positive feedback loop appears to be a part of the ''hard-wiring'' of infection that ensures rapid viral takeover of the cell. As infection progresses, the second promoter, at 38 map units, is transactivated by NS1 (Clemens and Pintel, 1988) and drives synthesis of the R3 transcripts, which use the same pair of alternative 5′ and 3′ splice sites present in the small intron region to regulate synthesis of the two primary capsid proteins, VP1 and VP2. In this case, a transcript that uses the downstream 5′ and 3′ splice sites encodes the minor VP1 polypeptide, translation of which initiates at a methionine codon between the two alternate 5′ splice sites. In the more abundant transcripts, which employ the upstream 5′ splice site, this initiation codon is spliced out, and translation of the major coat protein VP2 initiates from a start codon nearly 400 nts further downstream of the splice. Thus, the two primary translation products from the structural gene, VP1 (~83 kDa) and VP2 (~63 kDa), are expressed at a ~1:5 ratio. A third, more-truncated form of the VP2 polypeptide, called VP3 (~60 kDa),

is generated in full, but not in empty, particles by proteolytic cleavage of some 22–25 amino acids from the N-termini of the VP2 polypeptides, following their exposure on the particle surface.

While all parvoviruses encode both NS1 and one or more forms of NS2, only NS1, the replication initiator protein, is absolutely required for virus growth in all cell types (Cater and Pintel, 1992; Naeger *et al.*, 1990). NS1 functions in replication as an ATP-dependent, site-specific DNA-binding protein with DNA nicking and helicase activities, which allows initiation of DNA synthesis at specific viral origin sequences by introducing a site-specific single-strand nick. This provides a base-paired 3′ nt to serve as a primer for successive rounds of strand displacement DNA synthesis (reviewed in Cotmore and Tattersall, 2006a), while the transesterification reaction that creates the nick leaves NS1 covalently attached to the 5′ nt, where it is thought to recruit additional NS1 molecules to form the 3′-to-5′ replicative helicase.

However, parvoviral replication initiators have evolved into highly pleiotropic proteins, playing multiple roles in the viral life cycle. As mentioned above, in addition to their site-specific nicking function, they act as potent transactivators of viral gene transcription, binding to their recognition sequences in viral promoters and activating transcription through acidic C-terminal domains (Legendre and Rommelaere, 1994). In the MVM genome, NS1 binding sites are reiterated so frequently that any sequence of 100 base pairs or more contains a site, and some carry multiple tandem and inverted reiterations (Cotmore *et al.*, 1995). This suggests that NS1 might play a significant role in viral chromatin structure and/or progeny strand packaging. In contrast, NS2 polypeptides play indirect roles in supporting the MVM life cycle, modifying the cells of their natural murine host to support viral replication and mediate efficient capsid assembly. Advances in our knowledge of parvoviral DNA replication and packaging mechanisms have been reviewed extensively elsewhere (Cotmore and Tattersall, 2006a,b).

## III. RECOGNIZING THE TARGET: CELL SURFACE RECEPTORS AND VIRAL HOST RANGE

Parvovirus particles are extraordinarily rugged, remaining viable at room temperature for months, or years, and resisting desiccation or exposure to chaotropic agents. However, they also serve as covert delivery vehicles, able to gain access to the host cell cytosol and penetrate into its nucleus, where they lie in wait for it to initiate DNA synthesis as part of its own normal cell cycle. This reliance on the cell's unchecked transit into S-phase therefore suggests that the processes of parvovirus entry and latency remain largely undetected by their host's innate defense mechanisms.

This report focuses on both host range and cell entry mechanisms, since these topics are often intimately linked and informed by each other. Infection initiates through capsid-mediated binding to one or more glycosylated receptor molecule on the cell surface and is followed by virion uptake into the cell via receptor-mediated endocytosis. Transfer across the delimiting lipid bilayer of the entry vesicle into the cytoplasm is then affected by a capsid-borne phospholipase, and this is followed by delivery to, and entry into, the nucleus, where the viral genome is finally released from its protective shell. Thus, parvovirus genomes remain associated with their intact capsid throughout the entire entry process, and possibly even in primary viral transcription complexes, so that host cell–specific interactions with the viral particle could potentially impinge at multiple stages during the initiation of infection. While some parvoviruses exhibit narrowly restricted host ranges, others infect multiple host species and/or many tissues. Although such specificity can operate by disparate mechanisms, and be mediated either during entry or by cell type–specific differences in viral metabolism, two quite distinct patterns of capsid-controlled host range control have arisen in the genus *Parvovirus*, one exemplified by MVM, and the other by the FPV/CPV serotype. Whether these operate by similar mechanisms or even at the same stage in the entry process still remains to be determined.

Rather than interacting with a single cell surface receptor, many virus families employ two more-or-less separate classes of molecules: ''attachment'' receptors, or coreceptors, which simply accumulate virus in the vicinity of the cell surface; and infectious-entry receptors, which critically mediate genome transfer into the cell cytoplasm. Some members of the Parvovirinae are known to bind to a number of different cell surface molecules in ways that potentiate infection, although the extent to which they rely on multiple interactions appears to vary from species to species, and within a species from host cell to host cell, so that few general rules are apparent. Within the genus *Parvovirus*, members of the FPV serotype commonly bind to neuraminidase-sensitive *N*-glycolyl neuraminic acid side chains on some host cell types, but these presumably only function as attachment receptors, since infectious entry is insensitive to neuraminidase and is specifically mediated by binding to host species–specific protein domains on cell surface transferrin receptor (TfR) molecules (Parker *et al.*, 2001; reviewed in Hueffer and Parrish, 2003). In contrast, MVM binds to sialoglycoprotein receptor(s) present at about $5 \times 10^5$ copies per cell on murine fibroblasts, and both binding and infection are neuraminidase sensitive, indicating a critical role for specific oligosaccharide side chains in both of these steps. However, at present it is not clear whether one specific cell surface molecule mediates MVM entry, while others effect attachment, or if all $5 \times 10^5$ receptors are equipotent.

The clearest example of a receptor interaction dictating parvovirus host range is seen for FPV and its canine-tropic variant CPV, in Chinese hamster ovary (CHO)-derived TRVb cells, which lack any form of TfR. If feline TfR is expressed by transfection in these cells it allows efficient binding of CPV and FPV, leading to infection. In contrast, transfected canine TfR binds CPV capsids poorly, and FPV capsids not at all, and only allows infection by CPV (Hueffer *et al.*, 2003a). In this case, binding is specified by protein determinants on the receptor and involves several critical capsid residues that are arranged some 20–30 Å apart around the threefold spike, suggesting a broad region of receptor–capsid interaction. Remarkably, for CPV this interaction appears to be restricted to as few as one site per capsid rather than occurring at every 60-fold-related position (Hafenstein *et al.*, 2007; Palermo *et al.*, 2006). In contrast, MVM entry does not rely on interactions with the TfR, since MVM infects CHO TRVb cells efficiently without TfR transfection (Cotmore, S. F., and Tattersall, P., unpublished observations), but whether it establishes comparable interactions with other cell surface glycoprotein species is currently unknown. Irrespective of any such protein-mediated interaction, MVM host range is critically regulated by subtle, cell type–specific, interactions with sialic acid-containing oligosaccharides, which bind into the dimple-like depression at the capsid's icosahedral twofold axis. Below, we review details of what is known about receptor binding and host range constraints in these two disparate examples.

## A. The MVM model: Glycan-specific interactions around the twofold symmetry axes

MVM exhibits subtle strain-specific variations that allow different isolates to grow productively in murine cells of dissimilar differentiated phenotypes. Two independently isolated strains, termed allotropic variants, were initially identified: the prototype strain, MVMp, which grows productively in culture in fibroblasts such as the A9 cell line; and the hematotropic strain, MVMi, which replicates productively in T lymphocytes and hematopoietic precursors (McMaster *et al.*, 1981; Segovia *et al.*, 1991; Spalholz and Tattersall, 1983). Despite sharing 97% sequence identity and being serologically indistinguishable, these viruses are reciprocally restricted for growth in each other's host cell type (Tattersall and Bratton, 1983). In nonpermissive cells infection is restricted prior to viral gene expression (Antonietti *et al.*, 1988; Gardiner and Tattersall, 1988a), but both virus strains are known to compete for specific binding sites on the surfaces of both cell types (Spalholz and Tattersall, 1983), estimated to be present at $5 \times 10^5$ copies per cell on mouse A9 fibroblasts (Linser *et al.*, 1977; Spalholz and Tattersall, 1983). Following intranasal inoculation into newborn mice, MVMp is asymptomatic, and the virus remains confined to

the oropharynx (Kimsey *et al.*, 1986), while MVMi causes a generalized infection in which the main targets are endothelial cells, lymphocytes, and hepatic erythropoietic precursors, but where the pathological outcome varies with host genotype (Brownstein *et al.*, 1992).

The ability of MVMp to grow in fibroblasts was mapped *in vitro* using a selective plaque assay to two specific amino acids at positions 317 and 321 in the VP2 capsid protein sequence (Ball-Goodrich and Tattersall, 1992; Gardiner and Tattersall, 1988b). These lie at or near the particle surface, adjacent to the dimple-like depression that spans the icosahedral twofold axis of the virion (Agbandje-McKenna *et al.*, 1998). When a restriction fragment from MVMp differing at only these two VP2 residues (T317 and G321) was substituted into an infectious plasmid clone of MVMi (A317 and D321), the resulting virus was found to be >100-fold better at infecting fibroblasts than its parent (Gardiner and Tattersall, 1988b). In contrast, when either single change was introduced into MVMi separately, the resulting viruses showed at most a twofold increase in their ability to replicate in fibroblasts (Ball-Goodrich and Tattersall, 1992). This restriction, in turn, allowed the selection of second site mutants that could complement either of these changes (Agbandje-McKenna *et al.*, 1998; López-Bueno *et al.*, 2007). For each of the single mutants, multiple alternative second site mutations were identified, all affecting residues surrounding or extending down the sides of the twofold-related dimple. Surprisingly, if the MVMi backbone already carried the A317T mutation, complementing mutations in D321 were not selected, but instead the additional mutations D399G, D399A, V551A, or D553N were each found to effectively confer fibrotropism. In contrast, when the MVMi backbone already carried the D321G mutation, four of the six second-site mutants identified carried the MVMp A317T change, while in the other two, the coordinated mutations were S460A and Y558H. Thus, in an MVMi backbone, fibrotropism can be conferred by switching the side chains of a number of different residues that surround the twofold depression, suggesting that structural changes in this depression may mediate MVM cell type specificity. While little is know about the control of tissue specificity for most other parvoviruses, it is clear that amino acid changes involved in determining both PPV cell type specificity and virulence are also localized in this depression (Simpson *et al.*, 2002).

Lack of a lymphocyte plaque assay prevented the equivalent analysis of MVMp host range mutants in culture, but this has been effectively accomplished *in vivo* using adult immunodeficient SCID mice (Rubio *et al.*, 2005). Following intravenous injection of MVMp into such mice, this normally apathogenic virus strain was found to evolve through at least two distinct steps, the first of which conferred enhanced virulence, while the second generated complex shifts in host cell specificity and pathogenicity. During the early weeks of subclinical infection, injected MVMp viruses consistently segregated variants that showed altered,

large-plaque, phenotypes when tested *in vitro*, but retained the fibrotropic MVMp host range. However, unlike wild-type MVMp, when these variants were reinoculated into SCID mice via the oronasal route, they spread systemically from the oronasal cavity and were able to access, and replicate in, various major organs such as the brain, kidney, and liver. Genetic analysis of 48 of these clones consistently showed one of three single changes in the VP2 gene, V325M, I362S, or K368R. Both MVMp and the recombinant viruses could be detected in the bloodstream 1- to 2-day postoronasal inoculation and remained infectious when adsorbed to blood cells *in vitro*. However, wild-type MVMp was cleared from the circulation within a few days, while the viremia caused by the mutant viruses was sustained for life, leading to their being described as having higher ''virulence.'' Significantly, attachment of both mutant and wild-type viruses to an abundant receptor on primary mouse kidney epithelial cells could be quantitatively competed by wild-type MVMp capsids, suggesting that this enhanced virulence was not associated with major differences in receptor usage in the target tissues. However, productive adsorption of variants carrying any of the three mutations showed increased sensitivity to neuraminidase, when compared to wild-type virus, suggesting that the particles had a lower affinity for the sialic acid component of the receptor. This diminished affinity for sialic acid–bearing oligosaccharide chains was later confirmed by plasmon surface resonance studies, discussed below. This suggests that the selection of capsids with lower affinity for their cell surface receptors favors systemic infection, which may be a major evolutionary process in the adaptation of parvoviruses to new hosts.

As illustrated in Fig. 3, two of these virulence determinants, residues I362 and K368, are located on the wall of the dimple recess surrounding the icosahedral twofold symmetry axis, while V325 is positioned ~22 Å away in a threefold-related monomer, near the top of the depression. Consistent with this, the X-ray crystal structure of MVMp capsids soaked with sialic acid (*N*-acetyl neuraminic acid) showed the sugar positioned in this depression, immediately adjacent to residues I362 and K368. Thus, this likely identifies the position of the terminal sugar in the infectious receptor attachment site on the viral capsid. However, the equivalent phenotype seen in mutants carrying the V325M mutation suggests that this residue also modulates sialic acid binding in a manner similar to I362 and K368, even though it is physically somewhat distant (López-Bueno *et al.*, 2006). The depression at the twofold icosahedral axis of MVMp does extend toward the loop containing V325 from a threefold-related monomer, which interdigitates with the reference monomer, as shown in Fig. 3C. These observations therefore suggest that although sialic acid is an essential component of the receptor for MVMp infection, and it binds to capsid residues in the icosahedral twofold depression, the carbohydrate component of the surface receptor recognized by the virus may

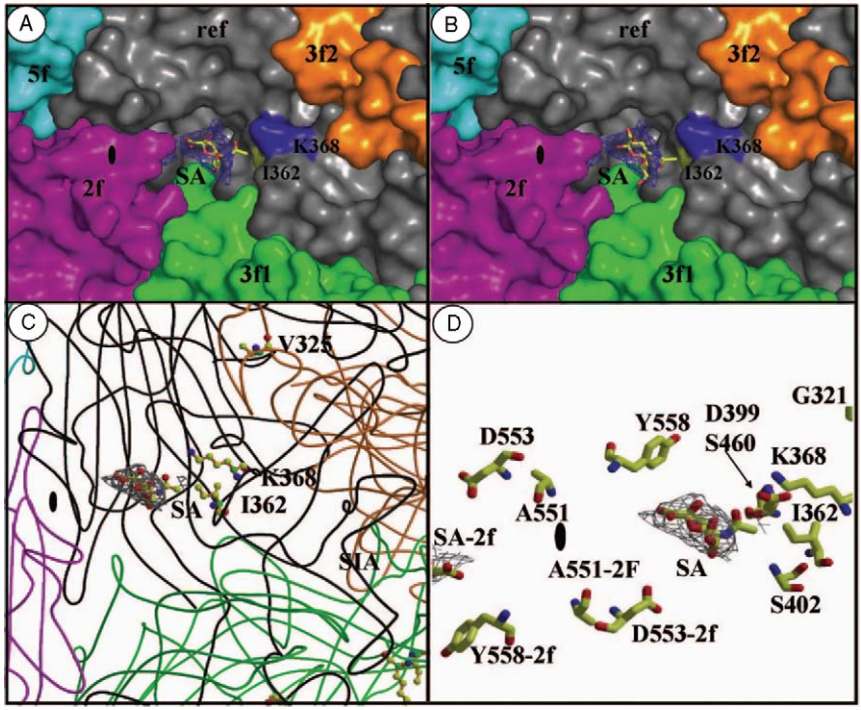


**FIGURE 3** Tissue specificity determinants lining the twofold dimple of MVMp: sialic acid (SA) binds in the dimple of the MVMp capsid, surrounded by residues involved in virulence. (A and B) Surface representations of a close-up of the depression at the icosahedral twofold axes of the MVMp capsid showing a reference VP2 monomer (ref, in gray), and icosahedrally related twofold (2f, in magenta), threefold (3f1 and 3f2, in orange and green), and fivefold (5f, in cyan) monomers. The surface positions of residues I362 and K368 are highlighted in yellow and blue, respectively. Residue V325 is not surface accessible. The SA model (colored according to atom type) is shown inside a $2F_O - F_C$ map, in blue, contoured at 1.8$\sigma$ in the two possible orientations of the carboxyl and *N*-acetyl groups of the SA molecule. (C) Coil representations of the ref, 2f, 3f1, 3f2, and 5f VP2 monomers, colored as in panels A and B. The positions and side chain atoms of residues I362, K368 (in the reference monomer), and V325 (in a threefold-related monomer) are shown colored according to atom type. The SA molecule is shown as in panel A, with the carboxyl group pointing down from the ring and the *N*-acetyl group pointing upward. (D) Close-up of the SA molecule (as in panel C) and residues on the wall of the twofold depression close to the binding pocket that either differ between MVMp and MVMi or confer fibrotropism on MVMi. The approximate location of the icosahedral twofold axes is shown by the filled oval. [Reproduced from López-Bueno *et al.* (2006), with permission. Copyright 2006, the American Society for Microbiology.]

be larger than a single sialic acid residue. Accordingly, a longer oligosaccharide might show additional contacts both within the dimple and adjacent to the loop carrying V325 at the top of this depression.

Evidence for enhanced interactions with longer, sialic acid–bearing oligosaccharides comes from glycan array and surface plasmon resonance studies (Nam *et al.*, 2006). These monitored the interactions of baculovirus-derived VLPs harboring the VP2 protein of MVMi, MVMp, the high-virulence MVMp mutants I362S, and K368R, or the double mutant I362S/K368R, with 180 different glycans. All of the particles bound specifically to oligosaccharide chains carrying terminal sialic acid residues linked 2–3 to a common Gal 1–4GlcNAc moiety. However, binding only occurred when the chains contained at least five saccharide residues and the binding affinity generally increased as a function of chain length. None of the VLPs recognized oligosaccharides with NeuAc α2–6 linked sialic acids, while MVMi was unique in binding efficiently to the four multisialylated glycans with α2–8 linkages that were present in the array, although the MVMp-derived K368R mutant also bound to one of these with lower affinity. This therefore supports a model in which the slight differences in topology and side chain interactions of specific residues lining the dimple, which can be seen in comparisons of the three-dimensional structures of MVMp and MVMi, reflect differences in the abilities of this cleft in each virus to accommodate somewhat different carbohydrate arrangements.

When reintroduced into SCID mice, these high-virulence MVMp mutants subsequently underwent pathogenic tissue-specific evolution, which again involved residues that map to the dimple (López-Bueno *et al.*, 2007). In this case, MVMp viruses carrying the I362S or K368R virulence changes, inoculated via the oronasal route, induced a lethal leukopenia after a 14–18 week delay, reflecting the pattern of disease typically found for MVMi infections within 7 weeks of infection. Sequencing the emerging MVM populations in these leukopenic mice prior to cloning identified consensus sequence changes at G321E and A551V in the I362S infections and at V575A and A551V in the K368R infections. Notably, changes at dimple residues 321 and 551 (indicated in Fig. 3) were among those previously identified in fibrotropic switch mutants selected by plaquing MVMi on mouse fibroblast monolayers. However, clonal analysis of the mutant populations from SCID mice revealed genetic heterogeneity at specific capsid residues, and only a few of these clonal isolates, which retained the parental G321 and V575 residues, were infectious *in vitro*. Rather, consensus genotypes were poorly infectious in culture, even in 324 K cells, an SV40-transformed human cell line that supports both lymphotropic and fibrotropic MVM variants, although virions could be generated following transfection of cloned genomes into these cells, indicating that later stages in the viral life cycle were

conserved. Virions from one such mutant, carrying the consensus mutations A551V and V575A, while unable to initiate infection in culture in a variety of different cell lines, rapidly induced lethal leukopenia when given to SCID mice, suggesting that *in vivo* this virus may exploit a subtly different allotropic interaction. This all suggests that the MVM dimple can be finely adapted to accommodate a range of different oligosaccharides and that, by changing the side chains and interactions of a small number of surface residues, the virus appears to be able to infect diverse repertoires of differentiated host cell types.

Other aspects of the viral life cycle clearly influence MVM's remarkable ability to switch its tissue specificity. In particular, the speed and efficiency with which heterogeneous virus populations are generated during parvoviral disease depend on high viral mutation rates, and resemble the generation of quasispecies typically encountered during the expansion of RNA viruses. Thus, for example, López-Bueno *et al.* (2003) observed that when MVMi-infected SCID mice received passive immunotherapy with a neutralizing monoclonal anti-capsid antibody, escape mutants, harboring single radical amino acid changes at tip of the threefold spike, emerged at high frequency ($2.8 \pm 0.5 \times 10^{-5}$). Such heterogeneity had not been previously expected for this DNA virus, which replicates using the normally high-fidelity DNA synthetic machinery of its host cell. However, similar mutation rates have now been observed for several members of the Parvovirinae (Badgett *et al.*, 2002; Shackelton and Holmes, 2006; Shackelton *et al.*, 2006), although the underlying causes remain conjectural. Thus, during a productive MVM infection, where high mutation rates are coupled with rapid virus expansion, generating up to $10^8$ infectious particles per infected mouse, specific virus strains may evolve rapidly, giving rise to host range mutants that are potentially able to infect an alternative set of differentiated cell types.

For MVM there is even further latitude for phenotypic expansion, since the ability of host range mutants to thrive in their new host cell can depend on the sequence, or even the expression level, of NS2, the minor viral nonstructural protein. As discussed above, when MVMi is adapted for growth in fibroblasts, the host range switch typically involves two coordinate mutations in the vicinity of the dimple. However, two host range switch mutants have been characterized that carry a single coding mutation at residue D399 in VP2, to alanine or glycine, together with a second, noncoding, guanine-to-adenine change at nucleotides 1970 or 1967, which influence the splicing patterns of the viral transcripts (D'Abramo *et al.*, 2005). When reconstructed into an infectious molecular clone of MVMi, all single mutants failed to replicate productively in fibroblasts, but viruses carrying a pair of mutations, with one of each type, were highly infectious. Specifically, the single D399 mutations allowed viruses to initiate infection in fibroblasts, but NS2 expression

was low, which led to poor accumulation and release of progeny virus. Mutations at 1967 or 1970 restored the MVMp splicing pattern, enhanced NS2 accumulation, and allowed efficient progeny production and release. Conversely, the D399 mutations destroyed the viruses' ability to initiate infection in EL4 lymphocytes. However, in lymphocyte infections, NS2 was expressed at high ratios even in the absence of upstream mutations, and progeny accumulation was efficient. Choi *et al.* (2005) showed that this requirement for different splicing signals to achieve optimal MVM NS2 levels reflects cell type–specific differences in RNA processing, which can thus impact host range. Exactly why high NS2 levels are required for efficient progeny virus production remains uncertain, and is probably multifactorial, but, in part, it appears to reflect a defect in capsid assembly seen in NS2 depleted cells (Cotmore *et al.*, 1997). This may suggest that it is difficult to assemble the single D399 mutants, but that either a second local capsid modification, such as A317T, or a boost in NS2 levels, eases this constraint. While wild-type NS2 is known to interact with the cellular nuclear export protein, Crm1 (Bodendorf *et al.*, 1999), remarkably, a mutation that promotes higher affinity Crm1 binding than wild type was also able to reverse this progeny production defect, so that even low-level expression of NS2 led to efficient virus expansion (Choi *et al.*, 2005). The high-affinity Crm1 binding mutant used in this study and several other similar mutations were first identified in SCID mice that had been infected with MVMi and exposed to neutralizing polyclonal antisera, in an attempt to protect the mice from leukopenic disease. These single or double amino acids changes in the NS2 Crm1 binding domain increased its ability to sequester Crm1 in a perinuclear locale, leading to an accelerated viral life cycle that somehow allowed the virus to circumvent the effects of neutralizing antibody (López-Bueno *et al.*, 2004). Taken together, this data indicates that mutations in NS2 that promote its efficient interaction with Crm1 can effectively modulate viral host range, by allowing a productive viral cycle to proceed in cells that would normally be nonproductive due to inadequate NS2 expression. Clearly, this provides a second example of how the virus's capacity for rapid evolutionary change can permit shifts in host range *in vivo*. Against this evolutionary force is ranged the extreme conservatism of this intensely compact virus, since most random mutations, or combinations thereof, appear to be incompatible with overall viral viability.

## B. The FPV/CPV model: Engaging the transferrin receptor at the threefold symmetry axes

In sharp contrast to the situation in MVM, where research has focused on analyzing changes in specificity for differentiated murine cell types, for viruses of the FPV serotype most attention has been directed at

understanding how the virus switched from being able to infect a number of carnivore species, excluding dogs, to being a potent canine pathogen. This event appears to have occurred early in the 1970s, when a complex virus mutant emerged and spread rapidly through the global dog population, erupting to pandemic status in 1978. This virus, called CPV-2, had lost the ability to infect cats. However, in 1979 an antigenic variant emerged, called CPV-2a, which can infect both host species and has since globally replaced the original virus in both domestic and wild dog populations. Phylogenetic analysis of DNA sequences suggests that all CPV isolates from dogs are derived from a single common ancestor, which only differs by a few nucleotides, some 0.4% of the genome, from the most recent common ancestor among the FPV-like viruses. Most of these changes have been conserved in the CPV variants emerging since 1978. All of the viruses from either cats or dogs replicate efficiently in feline cells in culture, but only CPV isolates infect dogs and cultured dog cells (Truyen and Parrish, 1992). The host range properties of CPV and FPV for both dogs and cats are controlled by multiple residues that map to disparate locales on or around the three-fold spike, as shown in Fig. 4. Primary control of canine host range is determined by residues at VP2 positions 93 and 323, which must be switched coordinately (Chang *et al.*, 1992; Horiuchi *et al.*, 1994; Hueffer *et al.*, 2003b; Llamas-Saiz *et al.*, 1996; Parker and Parrish, 1997; Strassheim *et al.*, 1994). Certain changes at residues 299 and 300 block the ability of the virus to infect dog cells, and changes in that region also appear to control the *in vivo* feline host range of CPV (Truyen *et al.*, 1994). The CPV-2a variant that emerged in 1979, which infects both host species, has additional changes at VP2 residues 87, 101, 300, and 305 (Parrish and Carmichael, 1986; Parrish *et al.*, 1988, 1991), and several other single mutations in CPV-2a have become widely distributed *in vivo* since 1980, including an N426D mutation that is present in the antigenic variant designated CPV-2b, which shares the CPV-2a host range (Strassheim *et al.*, 1994; Truyen *et al.*, 1995).

Some of the host range constraints of CPV and FPV seen in animals are reflected in tissue culture, where it is now clear that the block to infection by FPV in dog cells is primarily due to lack of a functional cell surface receptor. FPV and CPV both bind the feline TfR and use it to infect cat cells, but only CPV can bind to canine TfR. However, although CPV-2, CPV-2a, and CPV-2b all bind the canine TfR and infect dog cells, CPV-2 capsids bind to feline and canine cells much more efficiently and to higher levels than do CPV-2a or CPV-2b capsids, suggesting that CPV-2 forms different interactions with the TfR or binds to additional receptors on those cells (Hueffer *et al.*, 2003a). Thus, while VP2 residues 93 and 323 together control virus binding to the canine TfR (Hueffer *et al.*, 2003a), changes at VP2 residues 87, 300, and 305 in CPV-2a reduce receptor affinity and improve, in some way, the ability of the virus to use this receptor for infection (Hueffer *et al.*, 2003a; Palermo *et al.*, 2006).

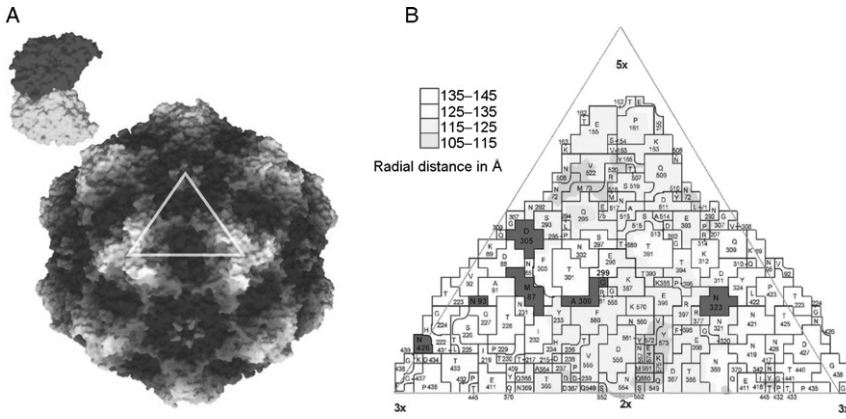


**FIGURE 4** Distribution of host-range determinant residues on the surface of CPV. (A) Surface-rendered model of the CPV capsid, viewed from above the dimple that surrounds the twofold symmetry axis, located on the bottom side of the triangle representing a single asymmetric unit, halfway between the threefold spikes. Toward the apex of the triangle lies the canyon surrounding the fivefold cylinder. A model of the ectodomain human transferrin receptor is shown at the same scale to indicate the relative size of the virus and its ligand on feline or canine cells. (B) A road map determined by the method of Rossmann and Palmenberg (1988) showing the surface exposure of VP2 residues in one asymmetric unit of the CPV type 2 capsid. The region shown comprises several symmetry-related VP2 subunits. Residues mentioned in the text that affect receptor binding or host range, and which differ naturally between FPV and CPV strains, are shaded. [Modified from Hueffer *et al.* (2003b) with permission. Copyright 2003, the American Society for Microbiology.]

TfR is a type II membrane protein that protrudes about 30 Å from the cell surface. The structures of canine and feline TfR have yet to be determined, but structural information is available for the human TfR, which is 79% identical to feline TfR at the amino acid sequence level. The human TfR consists of a large, butterfly-shaped, dimeric molecule with a span of about 100 Å and a molecular weight of 180 kDa. Each monomer has an apical domain, a helical domain, and a carboxypeptidase-like domain (Lawrence *et al.*, 1999), and mutagenesis of feline and canine TfRs indicates that both CPV and FPV bind to the apical domain. In confirmation of results from the *in vitro* cell binding assays, both FPV and CPV capsids were found to bind strongly to a recombinant form of the feline TfR ectodomain, while CPV-2b capsids bound much more weakly. In contrast, FPV capsids failed to bind at all to recombinant canine TfR (Palermo *et al.*, 2006), and while CPV-2 capsids bound the canine receptor, they did so only to very low levels, and CPV-2b binding was essentially undetectable. This binding pattern reflects the weak interaction seen in culture when the same receptor was expressed by transfection on otherwise TfR-negative

CHO cells, which nevertheless was sufficient to allow CPV-2b to be taken into and infect the cells. This low level of binding between canine TfR and CPV-2 or CPV-2b capsids, and its inability to bind FPV are in large part determined by minimal differences in the TfR apical domain, since simply changing residues 383 and 385 in canine TfR to their feline TfR counterparts allowed the mutant receptor to bind FPV to levels similar to those seen for the feline TfR, and likewise increased binding of CPV capsids. Residues 383 and 385 create a potential glycosylation site on canine TfR, which appears to be occupied *in vivo*, but the increased binding seen for the mutant is probably due to protein sequence, rather than oligosaccharide, changes, since enzymatic removal of N-linked glycans from the canine receptor did not lead to increased binding (Palermo *et al*., 2006).

The specific binding of CPV to canine TfR is thus controlled by several residues, positioned 20–30 Å apart on the ''high ground'' around the threefold spike, suggesting that a broad surface of the capsid interacts with the receptor (Govindasamy *et al*., 2003; Hueffer *et al*., 2003a,b). While less is known about the capsid residues that are involved in feline TfR binding, capsid mutations reciprocal to those which in CPV prevented canine TfR binding, at positions 93 and 323, did not appear to alter the binding of FPV to the feline TfR expressed on CHO TRVb cells, indicating that the canine and feline receptors make somewhat different contacts with these viruses (Hueffer *et al*., 2003a).

Asymmetric cryo-electron microscopic (cryo-EM) reconstructions, supported by quantitative *in vitro* binding studies, suggest a model in which the canine TfR ectodomain can bind to only one, or a few, of the 60 icosahedrally equivalent sites on empty CPV capsids, suggesting that these either have inherent asymmetry or that binding to their receptor induces asymmetry (Hafenstein *et al*., 2007). When a difference map, calculated by comparing the virus-receptor complex with the native virus, was superimposed on a stereographic projection of the icosahedral CPV surface structure, the known crystal structure of the human TfR ectodomain dimer (Lawrence *et al*., 1999) could be modeled into the additional cryo-EM density such that one of its two apical domains was in contact with the shoulder of one of the CPV spikes. In this model, the projected contact sites on the virus included residues that are known to control specific binding to canine TfR (Hueffer *et al*., 2003a).

Possibly, the restricted binding observed for the CPV–canine TfR interaction is due to inherent asymmetry in the empty particle, with one, or a few, distinct sites that have a conformation capable of binding TfR, whereas the other icosahedrally equivalent sites are slightly different. If so, this asymmetry must exist prior to genome encapsidation, and might indeed direct that process. This might happen if assembly is initiated around a special icosahedral fivefold vertex, which is the site of subsequent genome entry and exit, as is believed to occur in tailed

bacteriophage (Morais *et al.*, 2003). Alternatively, the final subunits to assemble may be sterically hindered from perfectly finishing the icosahedron, thus creating an asymmetric structural element at the capsid surface. However, it is also possible that TfR binding itself might induce asymmetry in an initially icosahedral particle, perhaps priming it for subsequent conformational shifts destined to occur during cell entry, as discussed below.

Thus it appears that after first adapting to dogs by acquiring changes that allowed it to bind canine TfR in a productive way, CPV has continued to evolve *in vivo*, acquiring additional mutations that lower its affinity for this receptor but enhance its ability to infect cells. Use of the TfR as the cellular receptor for these viruses also correlates well with the patterns of tissue specificity seen *in vivo*, as this receptor is highly expressed on crypt cells in the intestinal epithelium and on hematopoietic cells, which are the main target cells of CPV and FPV in animals (Parrish, 1995). However, TfR acts as more than a simple tether, dragging the capsid into the cell, since the precise interactions are important for successful cell infection, and some mutational changes in either the virus or the receptor allow capsid binding and cell uptake without leading to infection (Hueffer *et al.*, 2003b; Palermo *et al.*, 2003).

Transfer of the viral genome across the limiting lipid bilayer of its prospective host cell is one of the most challenging steps encountered during cell entry, and for many nonenveloped viruses this maneuver is so finely orchestrated that critical interactions required with cell surface receptor molecules play a major role in determining viral host cell specificity. To date, it is not clear whether any parvoviruses employ a receptor-orchestrated transfer mechanism of this type, but it is clear that they must undergo a specific structural transition after endocytosis, but before bilayer penetration, which leads to exposure of their VP1-specific ''entry'' peptide, VP1SR, and that inappropriate exposure of this peptide leads to their inactivation. Thus, it is tempting to speculate that interactions with specific receptors could modulate host range by allowing this transition to occur in a controlled way or in a favored locale that would be compatible with the transfer of a viable particle across the lipid bilayer, as we will now discuss.

## IV. BREACHING THE OUTER BARRIER: TO THE CYTOSOL AND BEYOND

Viral particles must function as rugged containers that protect the genome from environmental assaults encountered during transmission, but must also recognize and respond to a succession of specific cellular signals that allow them to navigate the complex entry portals of their host cell, and

ultimately deliver their nucleic acid to the appropriate replication compartment. Since parvoviral virions lack any accessory proteins, the component polypeptides of the nonenveloped capsid are the sole mediators of entry. While the capsid shell itself directs certain interactions, many other necessary contacts with cellular pathways rely on signal-rich N-terminal extensions present on VP1 and VP2 molecules. These are initially sequestered within the particle but are sequentially deployed at the virion surface during the cell exit and entry processes by a series of concerted conformational shifts in the capsid structure. Aspects of parvoviral entry have been reviewed by others in recent years (Vihinen-Ranta and Parrish, 2006; Vihinen-Ranta *et al*., 2004), but in this section we attempt to integrate data from a broader range of analyses. Specifically, we will examine the structural flexibility and transitions that viral particles are able to undergo *in vitro*, explore the structure of the VP1SR entry peptide, and finally consider vesicle trafficking and deployment of the entry peptide *in vivo*. This overview suggests that each step in the program of intracellular translocation of the intact particle to the cell nucleus is catalyzed by successively revealed motifs built into the capsid structure itself.

## A. Structural transitions in the virion induced *in vitro*

Empty parvovirus capsids are constructed from 60 copies of the capsid polypeptides, comprising, on average, 50 copies of VP2 and 10 copies of VP1. As diagrammed in Fig. 2, VP1 contains all of the VP2 sequence but has an extra, basically charged, 142-amino acid N-terminal extension, termed the VP1-specific region, VP1SR. The VP1 extension, shown in detail in Fig. 5A, is dispensable for both capsid assembly and DNA packaging, but is absolutely required for infectious entry, since it carries a phospholipase A2 (PLA2) active site essential for endosomal exit, as well as various clusters of basic amino acids and signaling motifs that may function at subsequent steps during nuclear localization. However, in MVM, only 547 amino acids from the C-terminus of the VP polypeptides are ordered, and therefore visible in the crystal structure, while the signal-rich N-terminal extensions, of 39 residues for VP2 and 181 residues for VP1, resist 60-fold averaging. These N-terminal regions are sequestered within the empty particle, but become sequentially externalized at specific steps in its life cycle, to modulate particle stability and to mediate successive interactions with the host cell.

In the viral particle, a cylindrical projection surrounds each of the 12 fivefold symmetry axes, and is itself encircled by a 15 Å-deep exterior depression, of unknown function, called the canyon. The cylinder is created by the juxtaposition of antiparallel β-hairpins from each of the fivefold-related capsid proteins. These β-hairpins are not interdigitated within the upper part of the resulting ''turret'' and so are potentially

flexible, and their organization in the crystal structure creates a narrow, 8 Å, central pore that penetrates through the virion shell to the particle interior. The tightest constriction in this pore is formed at its inner end by the juxtaposition of leucine side chains from VP2 residue 172 of five independent VP2 molecules. The phenotypic analysis of a complete set of amino acid substitution mutants at this highly conserved residue strongly suggests that L172 modulates the extrusion of VP1 N-termini (VP1NT) (Farr and Tattersall, 2004). All but one of these mutants produced DNA-containing virions, but only two, L172V and L172I, were infectious, the others being blocked for assembly, packaging, or viral entry. Several of the mutants were significantly defective for assembly at 39 °C, but not at 32 °C, and, while tryptic cleavage of their VP2 N-termini was normal, VP1 was degraded during *in vitro* proteolysis of mutant, but not wild-type, virions. The L172W substitution, while not significantly affecting assembly, effectively abrogated genome encapsidation, contributing to the emerging genetic evidence for both the *Parvovirus* and *Dependovirus* genera suggesting that one of these fivefold pores mediates encapsidation of the viral genome late in infection. For this step, the presumptive portal acts in concert with a viral helicase complex, which has been shown for AAV to be a small Rep protein, but, for the autonomous parvoviruses, is derived from NS1 in an unknown manner. It is currently not clear whether the packaging portal is physically distinct from the other 11 cylinders prior to being selected as the encapsidation point.

X-ray crystallography of MVM virions revealed ordered structure beginning at VP2 residue 40, which is on the inside of the shell, forming part of the basal structure that supports the cylinder. In full virions, but not in empty particles, the pore contains additional weak density, into which has been modeled a single copy of a conserved glycine-rich peptide that spans VP2 residues 28–38 (VP2 residue 28-GGSGGGGSGGG-38), shown in Figs. 1 and 5A. Additional density, corresponding to residues 36–39 from the remaining capsid proteins, extends back into the particle interior. Since, in the crystal structure, each pore accommodates a single glycine-rich peptide, only one of the five locally available VP N-termini can be externalized at any time. However, almost all of the VP2 N-terminal peptides become surface-exposed during entry, or during proteolytic digestion *in vitro*, suggesting that there are dynamic fluctuations in pore structure. Since the pore is only 8 Å in diameter, but must accommodate the passage of amino acids with bulky side chains during these extrusion events, this implies that the cylinder is an inherently dynamic structure. Indeed, one function of the canyon might be to provide space for the β-hairpins of the cylinder to move outward, thus allowing the pore to expand.

Viral genomes are packaged into some sort of preassembled empty particle, but evidence from AAV2 suggests that such particles are

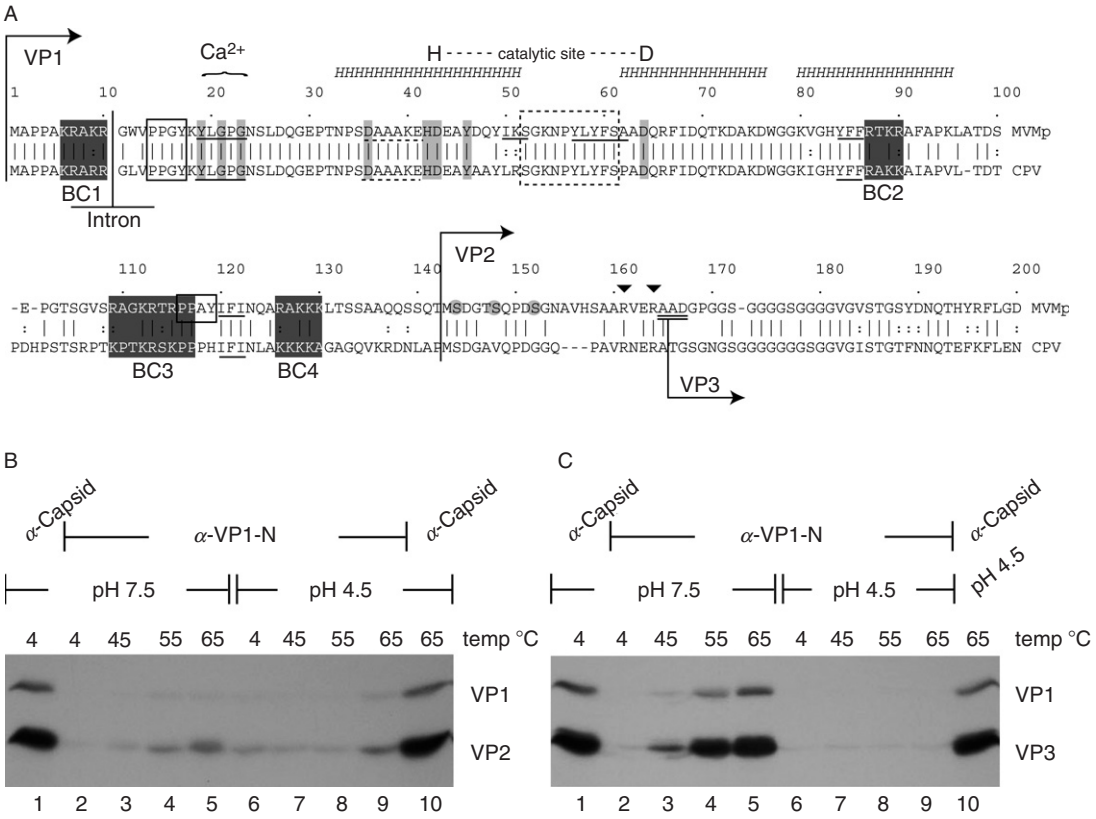
A
VP1
Ca2+
H ----- catalytic site ----- D
BC1
Intron
BC2
VP2
BC3
BC4
VP3
B
α-Capsid
α-VP1-N
α-Capsid
pH 7.5
pH 4.5
4 4 45 55 65 4 45 55 65 65 temp °C
VP1
VP2
1 2 3 4 5 6 7 8 9 10
C
α-Capsid
α-VP1-N
α-Capsid
pH 7.5
pH 4.5
pH 4.5
4 4 45 55 65 4 45 55 65 65 temp °C
VP1
VP3
1 2 3 4 5 6 7 8 9 10

somewhat specialized since they have to be assembled in the presence of the Rep proteins, which are the functional equivalent of the MVM NS1 polypeptide (Wu *et al.*, 2000). Both VP1 and VP2 N-termini are completely sequestered inside these empty capsids, but a structural shift occurs in the packaging complex prior to, or concomitant with, the beginning of DNA translocation, which allows a cohort of VP2 N-terminal peptides to emerge at the virion surface (Cotmore and Tattersall, 2005a). Whether these termini play a role in the packaging process remains uncertain, but they do appear to stabilize the final structure, as discussed below. These N-terminal extensions carry phosphoserine-rich export signals, which in some cell types direct packaged virions to be trafficked out of the nucleus prior to cell lysis (Maroto *et al.*, 2004). Full particles are thus released from the parental cell with all of their VP2 N-termini intact, but a third structural protein, VP3, is subsequently generated from most VP2 molecules by a proteolytic cleavage that removes 22–25 amino acids from its N-terminus. VP2 to VP3 cleavage can occur in the extracellular environment following release, but, if not, invariably occurs during entry into a new host cell (Clinton and Hayashi, 1975; Paradiso, 1984; Ros *et al.*, 2002). This cleavage can be mimicked *in vitro* by incubating virions with a broad variety of proteases, but the cleavage site appears flexible, and very accessible, so that it has been essentially impossible to totally ablate cleavage in MVM by mutagenesis or to stop it occurring *in vivo* using combinations of protease inhibitors (Clinton and Hayashi, 1975; Tullis *et al.*, 1992; Farr, G. A., Cotmore, S. F., and Tattersall, P., unpublished results). Since each pore can only accommodate one N-terminal peptide at a time, it is suggested that following proteolytic cleavage the residual

**FIGURE 5** Properties of the VP1 specific region. (A) Landmarks of the MVM VP1 N-terminus aligned with that of CPV, showing the basic clusters (shaded black), SH2 ligand motifs (single underline), SH3 ligand motif (dashed underline), PPXY motifs (open boxes), and individual PLA2 active site residues of the $Ca^{2+}$ binding and catalytic sites (shaded gray). The position of the minor splice intron is shown as an inverted "T," and the starts of VP1, VP2, and VP3 are indicated by arrows, and, in the latter case, potential N-terminal residues are double underlined. The serine residues phosphorylated in the VP2 N-terminus are circled in gray and the tryptic sites upstream of the VP3 N-terminus denoted by inverted carets (▼). Open, dashed box denotes conserved sequences unique to parvoviral PLA2s, between the predicted helices (*HHH*) bearing the catalytic histidine [H] and aspartic acid residues [D]. (B) Wild-type virions with intact VP2 N-termini (VP1/VP2 virions) were incubated for 10 min at the temperatures and pHs indicated, before buffer conditions were normalized and samples immunoprecipitated with antibodies that only react with intact virions (lanes 1 and 10), or with the VP1 N-terminal peptide (lanes 2–9). (C) Wild-type virions with cleaved VP2 N-termini (VP1/VP3 virions) were treated as in panel B. [Panels B and C reproduced with permission from Farr *et al.* (2006). Copyright 2006, the American Society for Microbiology. All rights reserved.]

glycine-rich sequence that is left in the pore is in some way retracted into the particle interior, and replaced by the intact terminus of a fivefold-related VP2. However, as mentioned above, the fivefold pores are quite narrow, and could not accommodate the bulky side chains that would need to be threaded through the cylinder from the particle interior, suggesting that each cylinder may be metastable. Remarkably, MVM virions carrying the single point mutations V40A, N149A, N170A, L172F, or L172T, located in the base of the cylinder, are stable as long as their VP2 N-termini remain intact, but become unstable when their VP2 N-termini are cleaved, disgorging their VP1SRs and genomic DNA at neutral pH (Farr *et al*., 2006; S. F. C. and P. T., unpublished results). This suggests a model in which the exposed VP2 N-termini act as ''guy-ropes,'' stabilizing the virion by preventing the metastable cylinder from undergoing a major structural rearrangement that is required for VP1SR extrusion, and which normally occurs at a later stage in entry. These point mutations apparently promote instability by lowering the activation energy required for this final transition. In this model, externally tethered VP2 N-terminal peptides stabilize the full virion, but cleavage of the resident cohort results in a transient conformational instability that allows concerted replacement of the cleaved peptides by a subsequent cohort of intact VP2 N-termini, which in turn restabilize the virion. Thus, the MVM structure would undergo several successive waves of destabilization and restabilization, until all of the available VP2 N-termini were cleaved, at which point the cylinders would exist permanently in the metastable state, poised to undergo the more drastic rearrangement that leads to extrusion of the VP1SR.

Although VP1 contains the same proteolytic cleavage site that is found in VP2, this is not accessible to digestion, and the VP1SR remains totally sequestered within the capsid during the early stages of entry. However, *in vitro*, the particle is capable of undergoing its second, more-extensive, rearrangement in response to controlled heating, discussed above, which allows exposure of the VP1SR without causing virion disassembly (Cotmore *et al*., 1999; Vihinen-Ranta *et al*., 2000; Weichert *et al*., 1998). In accord with the ''guy-rope'' model, freshly harvested, VP2-intact, virions are substantially refractory to this transition, but it is greatly facilitated, and rendered almost quantitative at neutral pH, by extensive proteolysis of VP2 N-termini to yield VP3, as documented in Figs. 5B and C, respectively, where transitioned particles are quantified by precipitation with antibodies directed against the VP1SR. Remarkably, this VP2 cleavage also renders the capsid transition highly pH dependent, so that it is impossible to induce under acidic conditions, at least just by heating. However, such pH-induced stabilization is entirely reversible, because once returned to a neutral environment, particles transition in response to

heat as if they had never experienced low pH (Farr *et al*., 2006). The VP2 cleavage thus resembles an activation cleavage step seen in a number of other nonenveloped virus families, where a previously stable virion is potentially compromised by a specific proteolytic event that facilitates subsequent exposure of a protein known to be essential for membrane penetration (Bubeck *et al*., 2005; Chandran *et al*., 2003). This allows the particle to exist in a metastable state, where the lowest energy form of the cleaved product is sequestered by the energy barrier between the two forms (Hogle, 2002). During entry, such viruses encounter some form of catalyst, such as low pH or an interaction with a specific receptor, which releases the metastable configuration, allowing the *de novo* exposure of sequences required for membrane penetration. Extensive proteolysis of the VP2 N-termini thus appears to play a comparable global role for MVM, in that it has a major effect on the stability of most particles in the population, strongly suggesting that it is likely part of a programmed entry mechanism. However, this cleavage has an unexpected outcome: it renders subsequent exposure of the entry peptide highly pH dependent, such that it occurs readily at neutral pH, but is effectively, but transiently, suspended in acidic environments. The structural basis for this enhanced stability at low pH remains to be detailed, and it may be that *in vivo* it is constrained by, for example, receptor interactions. Otherwise, it appears to indicate that the virion must access a neutral locale before it can undergo the type of programmed transition that is needed to expose its bilayer-penetrating PLA2 activity, and that this occurs as part of an authentic, and highly controlled, unfolding process, ultimately leading to productive infection.

In support of this model, heat-induced transition *in vitro* typically results in exposure of both the VP1SR and the viral genome (Cotmore *et al*., 1999; Farr *et al*., 2006; Vihinen-Ranta *et al*., 2002; Weichert *et al*., 1998), either of which would be irreversibly damaged within an obligate late endosomal/lysosomal entry compartment by exposure to hydrolases or depurinating acidic conditions. Enhanced virion stability at low pH could thus serve to protect these sensitive elements as the particle is trafficked through hazardous entry compartments into a more favorable vacuolar microenvironment. Alternatively, although apparently closely linked *in vitro*, exposure of the VP1SR and viral genome might be part of a multistep process *in vivo*, triggered sequentially by different stimuli in the entry pathway.

Suikkanen *et al.* (2003b) drew substantially different conclusions concerning the significance of particle acidification during CPV entry. They observed that CPV particles exposed to pH 4–6 *in vitro* developed measurable PLA2 activity, which persisted when virions were returned to neutral pH. Accordingly, they suggested that low pH could provide

an essential activation step in virion maturation preparatory to cytoplasmic entry, which correlated with immunofluorescence studies of virion uptake, discussed later, that show exposure of VP1NT in a cellular lysosome-like compartment. However, the study does not report what proportion of CPV particles became structurally rearranged, or whether they remained infectious. It is possible, therefore, that this observation corresponds to the enhanced VP1 accessibility seen for a small proportion of MVM VP2-intact virions following exposure to pH 4.5 (compare lanes 2 and 6 of Fig. 5B), and which is not seen in VP2-cleaved particles (compare lanes 2 and 6 of Fig. 5C). According to the alternative, ''low pH-stabilization model,'' developed here, any particles in which these sequences were exposed prematurely would be unlikely to progress correctly through the rest of the programmed sequence, and any particle in which they became exposed in an acidic environment, would, in any case, be inactivated. Such low-pH-induced activation would also be surprising, and counterintuitive, in any virus that, like CPV, transits through the gastrointestinal tract of its host. However, further experiments will be needed to clarify whether these disparate findings represent a significant biological difference between CPV and MVM.

Ultimately, the genome may well be extruded *in vivo*, as it is *in vitro*, but still remain attached to, and possibly sequestered by, the particle. Prolonged storage of VP2-cleaved MVM virions at 4 °C does lead to exposure of both VP1SR and the genome in an increasing proportion of otherwise intact particles. However, strong interactions between the left-end hairpin of the DNA and the transitioned particle keep these two elements together. Attempts to recapitulate this type of measured transition *in vitro*, just using heating steps, have proven equivocal, but it is possible to bind the left-end hairpins of MVM to intact particles *in vitro* (Willwand and Hirt, 1991), so that perhaps physiologically induced transitions might preserve such interactions.

## B. Essential elements in the VP1-specific entry peptide

During infection, VP1 molecules are transported into the nucleus as part of a trimeric assembly intermediate, comprising one VP1 and two VP2 molecules, which are then further assembled into empty particles (Riolobos *et al*., 2006; Valle *et al*., 2006). However, whether these heterotrimers are distributed throughout the particle so that there is one VP1SR at 10 of the 12 fivefold symmetry axes, or are clustered in some other way, remains uncertain. The sequence of the MVM and CPV VP1 N-terminal regions are shown in Fig. 5A, with the positions of the VP2 start sites and the predominant VP2-to-VP3 cleavage sites indicated. The 142-amino acid VP1SR contains at least three distinct elements: (1) a short N-terminal peptide that contains a consensus nuclear localization sequence (NLS)

dubbed BC1, (2) a PLA2 domain of around 70–80 amino acids that is highly conserved among the Parvoviridae, and (3) a second stretch of some 70 amino acids, which carries a series of basic amino acid clusters (BC2–BC4) that resemble conventional NLS, and, in MVM, also contains a PPXY motif that is essential for infectious entry. As can be seen in Fig. 5A, the VP1SR also contains several putative *src* homology (SH) interaction domains, to which no function has yet been ascribed. Unfortunately, to date we have no structural data for the VP1SR positioned either inside the particle or following its extrusion to the virion surface. It is quite likely that this peptide domain may need to unfold and refold during transit, to navigate its exit portal, and while the conserved PLA2 module is clearly essential for infection, the exact limits of this functional unit have not been determined. It is thus possible that the inboard ~70-amino acid peptide, which spaces the PLA2 sequences from the VP core, may also play a structural role in the folding and disposition of this essential enzyme, or may function as a ''stem'' to position the PLA2 active site at an optimal orientation and distance from the virion surface.

### 1. The PLA2 domain

The conserved PLA2 domain, containing a sequence of ~60 amino acids that can be modeled into a characteristic PLA2 helical fold, is present in most Parvoviridae, generally occupying a region near the extreme N-terminus of VP1. First identified by Zadori *et al.* (2001), this element is expressed in seven out of the nine genera in the family Parvoviridae, while no other virus families are currently known to possess such an activity (Tijssen *et al.*, 2006). The exceptions within the Parvoviridae are *Aleutian mink disease virus*, the single member of the genus *Amdovirus*, and members of the *Brevidensovirus* genus of insect parvoviruses. Phospholipases are classified according to the position of the ester bond they hydrolyze in the glycerol backbone of their phospholipid substrate, with PLA2 enzymes cleaving fatty acids at the sn-2 position. Parvovirus PLA2s require millimolar $Ca^{2+}$concentrations for catalysis, which groups them with a large class of extracellular or secretory enzymes (sPLA2s) rather than with intracellular species. Parvoviral PLA2s comprise a novel subfamily, Type XIII, of the secreted PLA2 (sPLA2) superfamily (Balsinde *et al.*, 2002; Brown *et al.*, 2003), which contain a YxGxG $Ca^{2+}$ binding site and a histidine/aspartic acid active site, as shown in Fig. 5A. Where structural details are known, the active site H and D residues in sPLA2s are situated on apposing α-helices, which are usually held in a parallel orientation by a number of disulfide bonds (Berg *et al.*, 2001). Indeed, these small proteins are remarkable for the number of cysteine residues they contain—that is, except for the parvoviral enzymes, which contain none. It seems likely that this absence of disulfide bonds reflects the extraordinary requirement for parvoviral PLA2s to be translocated from

the inside to the outside of the virion. The viral enzymes are also distinguished by being more compact than other subtypes, particularly in the loop between the two α-helices carrying the active site residues, which is normally 20–40 residues long, but is truncated to ~10 residues in the parvoviral PLA2s, with several of these being highly conserved across the parvoviral genera. Remarkably, PLA2s from different parvovirus genera can vary in specific activity by 1000-fold, but all exhibit resistance to most specific sPLA2 inhibitors and low phospholipid polar head group specificity (Canaan *et al.*, 2004), perhaps as a consequence of the relative lack of rigidity predicted from the absence of disulfide cross-links. Accordingly, parvoviral PLA2s exhibit broad substrate specificity *in vitro*, hydrolyzing phosphatidyl-glycerol, phosphatidyl-choline, and phosphatidic acid with high efficiency, phosphatidyl-ethanolamine and phosphatidyl serine somewhat less well, and phosphatidyl-inositol poorly. These enzymes can therefore attack the outer leaflet of mammalian cell bilayers (Tijssen *et al.*, 2006). They have pH optima between 6.0 and 7.0, and require concentrations of calcium that are typically ~10,000 times those found in the cytosol (the $^{Ca}K_d$ for the PPV enzyme is 1 mM), suggesting that they are unlikely to function in this environment. How the apparently globular viral PLA2 polypeptide transits an ~8Å channel in order to function in endosomal escape remains enigmatic. Given that these enzymes lack disulfide bridges, it may be that this feat is achieved by both the directional unfolding and refolding of the enzyme, as well as by the opening of the pore at the fivefold vertex. This would allow the bulkier side groups of the random coil form of the polypeptide to reach the exterior of the virion, where it could refold to an enzymatically active form.

### 2. Nuclear localization motifs, basic clusters, and PPXY motifs

Capsid proteins must be transported into the cell nucleus twice during the viral life cycle, first as trimeric assembly intermediates following synthesis, and then again during cell entry, to traffic the incoming viral genome into the nucleus. Lombardo *et al.* (2002) identified four clusters of basic amino acids in the VP1SR of MVM that conform to conventional NLS sequences, as shown in Fig. 5A, and showed that two of these, BC1 and BC2, as well as a nonconventional structural domain in VP2 referred to as a nuclear localization motif (NLM), were able to target individually expressed VP proteins to the nucleus. Peptides containing the BC1 equivalent from CPV (6-KRARR-10) could also transport foreign proteins into the cell nucleus, while changing individual basic residues to glycine, impaired such transport (Vihinen-Ranta *et al.*, 1997). Introducing these mutations into an infectious plasmid clone gave virus with diminished infectivity, suggesting that BC1 might also be involved in transporting

incoming CPV virions to the nuclear pore (Vihinen-Ranta *et al.*, 2002). However, direct associations with members of the cellular karyopherin family of shuttling transport factors, which would be expected to mediate such processes, have yet to be demonstrated, and the BC1 motif is positioned immediately next to conserved PLA2 sequences, so that major substitutions in the MVM BC1 do compromise PLA2 activity (Farr, G. and Tattersall, P., unpublished results), and hence impair virion infectivity for a different reason. Thus, at present, the trafficking role of BC1 during virion entry remains uncertain. In contrast, while the entire region between BC2 and BC4 could not be deleted without destroying infectivity (Lombardo *et al.*, 2002), BC3 and BC4 did not behave like NLS as part of microinjected peptides (Vihinen-Ranta *et al.*, 1997), and did not show transport activity for VP1 either expressed alone or in the context of the MVM genome (Lombardo *et al.*, 2002), so that their role in the viral life cycle remains obscure.

Comparisons with the VP1 and VP2 N-termini of AAV2, which together constitute a region equivalent to the parvovirus VP1SR, highlight the complex nature of this region. Thus, while AAV2 similarly deploys these sequences to mediate virion entry, the peptides have no NLS activity in the position of BC1 (Sonntag *et al.*, 2006). However, they do retain both the PLA2 module and a 70-amino acid sequence containing three basic clusters in approximately the positions of the parvovirus BCs 2 through four motifs. Notably, the last two motifs are represented in the virion both as part of approximately five PLA2-bearing VP1NT, and also as part of five VP2 N-termini, which, like VP1NT, can become exposed at the virion surface *in vitro* during a heat-induced transition (Grieger *et al.*, 2006; Sonntag *et al.*, 2006). While VP2 forms are not absolutely essential for AAV2 infectivity, the expression of these two basic motifs on a discrete extension suggests that the sequence does not merely serve as scaffolding for the PLA2 domain. Rather, it appears to perform some specific function, as it would if, for example, it provided additional signals that enhance VP1-mediated nuclear trafficking. Alanine scanning mutagenesis directed at the three basic motifs effectively impaired the infectivity of the resulting particles (Wu *et al.*, 2000), as did substitution of glutamic acid for three of the basic residues in each motif (Sonntag *et al.*, 2006), but substituting asparagine for two basic residues in the first two motifs gave infectious virus, indicating that these two motifs may not individually constitute critical nuclear homing signals. In contrast the third motif (166-PARKRLNF-173) in AAV2, called BR3 by Grieger *et al.* (2006), was inactivated by the double asparagine substitution. Significantly, this mutant retained functional PLA2 activity, and simply substituting the BC1 NLS from CPV (4-PAKRARR-10) for the mutated sequence, restored infectivity, suggesting that this cluster might well be implicated in virion

trafficking. However, Sonntag *et al*. (2006) could not detect transport activity associated with this peptide or with the longer sequence, 160-GKAGQQPARKRLNF-173, following microinjection, although peptides representing the first two basic clusters did mediate nuclear transport. Thus the available evidence is conflicted, but the strong conservation of spaced basic clusters, together with the negative effects of mutations and deletions in this complex region, indicate that it has some sort of essential role(s) in entry, possibly involving nuclear trafficking.

In MVM there are also two PPXY motifs in the VP1SR, one (6-KRAKRGWVPPGY-17) positioned just downstream of BC1 and the other (109-RAGKRTRPPAY-119) overlapping BC3. PPXY motifs could potentially influence trafficking because this sequence binds a subgroup of cellular ''WW'' domain-containing proteins. WW domains form a large family of interaction modules, which mediate a wide range of protein–protein interactions in complex regulatory networks in the cell. For example, PPXY motifs control the trafficking of some cell surface receptors following endocytosis and orchestrate interactions with the class E vacuolar protein sorting machinery, which directs trafficking to the multivesicular body. This motif can also mediate ''late domain'' functions in enveloped viruses, directing the final pinching-off step during progeny virus budding. Such interactions are generally inactivated by mutating the PPXY tyrosine to alanine, and when introduced into either of the MVM sites this mutation severely impaired virion infectivity (Farr, G. and Tattersall, P., in preparation). However, the BC1-proximal mutation also inactivated the viral phospholipase so that its significance for other steps in entry is hard to assess. In contrast, the BC3-proximal mutant retained PLA2 activity, and could complement PLA2 knockout virions for entry, but could not itself be complemented, even by wild-type virus. This suggests that it is likely required *in cis* with the incoming virion and operates at a point in the entry process that is downstream of the PLA2 function. All other members of the genus *Parvovirus* lack a perfect VP1SR PPXY motif in the BC3-equivalent position, for instance, in both FPV and CPV this sequence is 117-PPPH-120. However, the exact sequence constraints that operate on the consensus remain uncertain, so that this region of the VP1SR may also play motif-driven trafficking or interaction roles in other parvovirus entry pathways.

## C. Endocytosis, vacuolar trafficking, and structural transitions *in vivo*

Relatively little is known about parvovirus infectious entry pathways, in part because productive and nonproductive routes are difficult to differentiate. Particle-to-infectivity ratios are in the order of 300:1 for

MVMp and ~1000:1 for CPV, with most of the incoming particles failing to navigate the entry compartments successfully, so that ultimate translocation into the nucleus is a rare event. Vesicle trafficking is complex, and its study is further complicated by the observation that particles are delivered to many different cell locations, including both recycling and degradative compartments. Many studies typically compound these problems by using high multiplicities of input virus to facilitate signal detection, but trafficking pathways within the cell can be modified by cargo overload or drug treatments. Consequently, much of the internalized virus appears to enter dead-end pathways that cannot provide the genome access to the nucleus, perhaps becoming structurally modified and/or inactivated *en route*. In such situations, comparison with mutant viruses that have specific, known, entry defects can be illuminating. For example, Fig. 6 shows by immunofluorescence confocal microscopy that 8 h after binding the intracellular distribution of wild-type MVMp appears identical to that of a PLA2 mutant known to be unable to exit from its vacuolar entry portal. Thus, essentially all observable wild-type viruses appear to be retained within the cell's vacuolar network, and

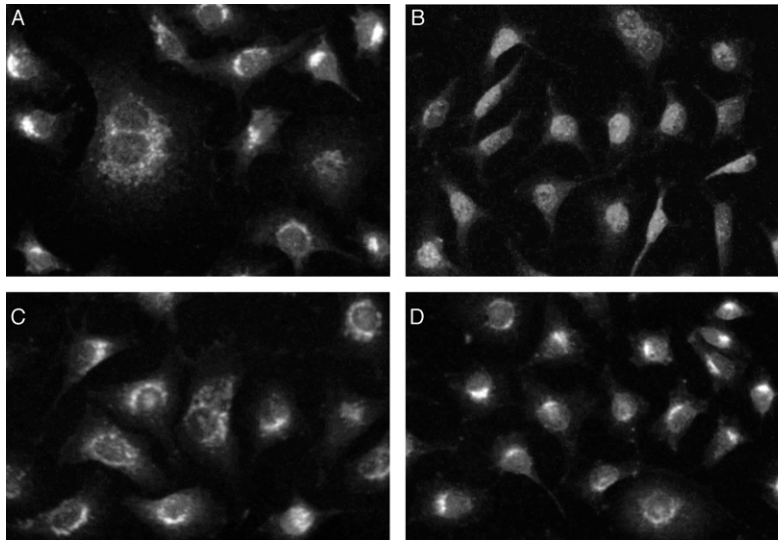


**FIGURE 6** Intracellular distribution of incoming virions. A9 cells infected with 500,000 wild-type (A), H42R (C), or ΔVP1 (D) virions per cell, fixed 8 h postinfection and stained with a monoclonal antibody specific for intact capsids. Cells shown in panel B were infected with wild type as in panel A, except that Type V neuraminidase (100 μg/ml) was added to the medium during infection. Images (1-μm sections) were acquired on a Zeiss LSM 510 laser scanning confocal microscope. (Reproduced with permission from Farr, Ph. D. thesis, 2005.)

could be earmarked for recycling or degradation rather than infection. To be biologically significant, entry steps must be seen to lead to productive infection, but for parvoviruses the first readily measurable indicator of successful initiation is the expression of NS1, a significantly late event that requires prior viral DNA synthesis and transcription. Moreover, for these viruses to initiate infection, the host cell must enter S-phase of its own volition so that any experimental intervention that slows or inhibits progress through the cell cycle may artifactually appear to interrupt the entry process. Accordingly, studies involving inhibitory drugs that are more-or-less specific for particular cellular interactions, or the delivery of mutant or overexpressed cellular control proteins, represent an area of considerable interpretive challenge.

Following receptor binding, all parvoviruses are rapidly internalized from the cell surface by receptor-mediated endocytosis, predominantly via clathrin-coated pits, and enter an endosome compartment that is sensitive to lysosomotropic agents such as bafilomycin A, indicating that low endosomal pH is somehow essential for infection. However, members of the genus *Parvovirus* remain sensitive to bafilomycin A for many hours after internalization, indicating that the required trafficking scheme may be complex and/or the penetration process inefficient. Such exposure to low pH during entry might be required because it induces essential conformational changes in the virion, because the viruses specifically need to transit a hydrolase-rich late endosomal/lysosomal compartment to accomplish an essential cleavage event, or because the ability to generate low pH compartments is absolutely required for the cell to sustain the required endosomal trafficking patterns. How many of these possibilities pertain is currently unclear and could vary between viral species. For MVM, endosomal proteases are known to generate VP3 polypeptides from VP2 molecules following engulfment (Mani *et al*., 2006; Ros and Kempf, 2004), which is likely important because it both removes the nuclear export signals in the VP2 N-termini (Maroto *et al*., 2004) and primes the virion for its subsequent conformational transition (Farr *et al*., 2006). The need for this modification thus supports immunofluorescence analysis of internalized particles and studies with inhibitory drugs (Ros *et al*., 2002; Suikkanen *et al*., 2002) in suggesting that infectious entry probably occurs via a late endosomal or lysosomal route, since these compartments are rich in proteases and nucleases. Such exposure would also explain how genomes lose their covalently linked NS1 molecules, and the nucleotides of the ''tether'' DNA sequence, prior to arrival in the nucleus. Exposure to acidic conditions *in vitro* also influences particle stability, as discussed in detail in Section IV.A , perhaps protecting essential acid or hydrolase-sensitive viral structures within an obligate late entry compartment or mediating other required rearrangements. Finally, vesicle trafficking is a protracted and potentially flexible process that leads to

particle delivery to many different cell locations. This complexity is illustrated by studies with CPV, which appears to remain physically associated with its receptor, TfR, for at least 4 h after internalization, since infectious entry can be blocked throughout this period by intracytoplasmic injection of antibodies directed against the cytoplasmic tail of the receptor (Parker *et al.*, 2001). The normal cellular uptake and complex recycling patterns of TfRs have been well characterized, and are known to depend on the presence of a YTRF (Tyr-Thr-Arg-Phe) motif in its cytoplasmic tail. However, when these sequences were deleted or mutated, or polar residues introduced into the TfR transmembrane domain, which vastly increased receptor degradation, virus infection efficiency was unaffected (Hueffer *et al.*, 2004), suggesting that infectious entry for CPV may involve a minority of TfRs that take-or are induced by bound virions to take-a rare pathway.

For MVM, the kinetics of intracellular VP2-to-VP3 cleavage, and of VP1SR and DNA exposure for the bulk particle population, have been tracked within cellular entry vesicles by immunofluorescent staining and *in situ* hybridization (Mani *et al.*, 2006). These changes were not conspicuously triggered by interactions with cell surface receptors, but became detectable, apparently simultaneously, within minutes of internalization in early endosomes, and could be blocked by preventing endosomal acidification with chloroquine or bafilomycin A. Remarkably, these authors observed VP1SR extrusion from both empty and full virus populations, occurring with similar kinetics. Since such VP1SR exposure is never seen if empty particles are heated *in vitro*, this might suggest that prior interactions with the cell had modified their structure, or led to their fragmentation. Suikkanen *et al.* (2003b) observed that VP1SR exposure from CPV virions increased with time between 1- and 8-h postinfection, and such forms colocalized with intact capsids in perinuclear lysosomes, whether or not the cells were treated with acidification-blocking drugs. While relatively few TfRs were detected in lysosomal vesicles in uninfected cells, throughout the course of CPV infection intact virions colocalized with TfRs, first in vesicles that resembled recycling endosomes, but later, by 8-h postinfection, in perinuclear lysosomes, perhaps suggesting that the virus had modified the cycling pathway of its receptor. Signal from exposed MVM genomes also colocalized with intact capsids in successive endosomal compartments, progressively accumulating for around 8 h after internalization, but by 21 h, although perinuclear vesicles remained loaded with intact capsid particles, little exposed viral DNA remained. Unfortunately, the fraction of the total endosomal virion population that contributes to the colocalizing signals cannot be assessed in this kind of microscopic analysis, and may be quite limited. It also seems likely that, given the relative inefficiency with which infection is initiated, the great majority of observed shifts in particle structure may reflect their degradation rather than their participation in a

productive infectious entry pathway. Nevertheless, such observations do illustrate that some transitions that have been documented *in vitro*, do also occur *in vivo*.

Within a few hours of internalization, both infectious virions and entry-defective mutants or empty particles are similarly trafficked to large, extranuclear, crescent-shaped clusters of vesicles that are focused on one side of the cell nucleus, as seen in Fig. 6. These resemble, and likely are, microtubule organizing centers since many of the vesicles appear to be lysosomes, and the processing of early endosomes to late endosomes/lysosomes requires their movement along microtubule networks. Accordingly, Parker and Parrish (2000) showed that overexpression of a dominant interfering mutant of dynamin altered trafficking of CPV-containing vesicles such that the concentration of input virus in perinuclear vesicles was significantly inhibited. Likewise, Vihinen-Ranta and colleagues (Suikkanen *et al.*, 2002; Vihinen-Ranta *et al.*, 1998), showed that the microtubule-depolymerizing drug nocodazole inhibits productive infection and leaves vesicular structures containing CPV near the cell periphery. In a classic study of transcytosolic vacuole trafficking, Heuser showed that shifting the extracellular medium of fibroblasts from pH 7.5 to 6.8 caused many perinuclear late endosomes/lysosomes to return to the cell periphery, in a nocodazole-dependent reaction, that could be reversed, mediated again by microtubules, by returning the cells to neutral pH (Heuser, 1989). Similarly, we have found that perinuclear clusters of MVM virions can be disrupted and scattered toward the cell periphery by exposing cells to low pH, in a reaction that can be blocked by nocodazole, but these return rapidly to their original location if the extracellular pH is returned to neutral, again in a nocodazole-dependent fashion. Thus many of the virus-filled vacuoles that occupy these perinuclear crescents appear to be typical late endosomes/lysosomes, pursuing their normal trafficking pathways. Microinjection of antibodies to dynein caused CPV vesicles to remain peripheral, supporting a model in which this motor protein drives microtubular transport of CPV entry vesicles.

MVM virions in perinuclear crescents disperse with time and much internalized virus is recycled back to the cell surface, where it can be released by the receptor-destroying enzyme, neuraminidase. Thus, for example, in one quantitative multiplex PCR analysis, populations of synchronized A9 cells infected for 6 h at 37 °C with 500 genomes per cell of either wild-type or a PLA2-negative mutant MVM, and then incubated in neuraminidase for an hour to ensure removal of all cell surface–bound virus, subsequently recycled approximately two-third of the remaining, intracellular, genomes back into the neuraminidase-supplemented medium during an overnight incubation, without evidence of accompanying cell death (S. F. C. and P. T., unpublished results). Clearly, these virus particles had failed to navigate the necessary infectious entry pathway.

Exactly where infecting viruses penetrate the endosomal bilayer is uncertain, but CPV infectivity can be blocked by the intracytoplasmic injection of antibodies directed against structural epitopes on the capsid or VP1SR-specific sequences, indicating that there must be an essential, capsid-associated, cytoplasmic phase, and that exposure of the VP1SR must accompany or precede infectious entry into the cytoplasm (Vihinen-Ranta *et al.*, 2000, 2002). Labeled dextrans with molecular radii of ~3000 were progressively released into the cytosol 8–20 h after they are codelivered to the cell with CPV virions, while dextrans of Mr 10,000 were retained in vesicles. This may suggest that CPV infection does not lead to disruption of the endosomal vesicles, but does induce a permeability change in their membranes (Suikkanen *et al.*, 2003b). Thus, although the effects of co-uptake with PLA2-defective virions were not explored in this study, the observed permeability increase might reflect viral enzyme activity. Complementation analysis between wild-type and mutant particles has been used to show that bilayer penetration does require deployment of this lipolytic PLA2 function (Farr *et al.*, 2005). These studies used an MVM mutant with a single H42D amino acid substitution in its PLA2 active site, which severely impaired its enzymatic activity and abrogated its infectivity. However, the mutant phenotype could be complemented in *trans* by coinfection with wild-type or mutant virions, provided they expressed functional PLA2, but not by wild-type empty particles, even though these carry sequestered VP1SR sequences. The H42R mutant was also complemented by polyethyleneimine-induced endosome rupture or by coinfection with adenovirus, as long as uptake of the two viruses was simultaneous and the adenovirus was capable of deploying pVI, a capsid protein with endosomolytic activity. Thus MVM, and likely other members of the genus, appears to use its capsid-tethered phospholipase activity to penetrate the endosomal membrane. If this event is successful, infection with the H42R mutant then proceeds normally, suggesting that, for MVM at least, transiting the endosomal membrane is the only step during infection that requires such potent phospholipase activity. However, since the PLA2 activity of the mutant virus was compromised, rather than destroyed, it remains possible that this diminished activity could be sufficient to support additional roles for the enzyme in the viral life cycle.

## D. From cytosol to nucleus

Since CPV infectivity can be blocked by the intracytoplasmic injection of antibodies directed against both intact capsids and the VP1-specific sequences (Vihinen-Ranta *et al.*, 2000, 2002), genomes associated with such forms must at least enter the cytoplasm during the normal course of infection. For AAV2 it has also been shown that monoclonal antibodies with equivalent specificities injected into the cell nucleus similarly block

infection, providing the first functional evidence that, at least for this virus, a transitioned capsid is present throughout the cytoplasmic and nuclear translocation phases, and is implicated in nuclear functions (Sonntag *et al*., 2006). In support of this interpretation, CPV virions microinjected into the cytoplasm were found to translocate into the nucleus intact, as demonstrated by their reactivity with structure specific antibodies, where they successfully initiated NS1 expression within 24 h (Suikkanen *et al*., 2003a; Vihinen-Ranta *et al*., 2000). Microinjected empty capsids were similarly transported, but whether any of this movement was VP1SR-driven remains uncertain. Notably, whereas karyopherin-mediated entry via the nuclear pores is typically rapid, viral transport in the CPV studies was slow, with few particles entering the nucleus within 3 h of cytoplasmic injection, although these became apparent in 40–50% of injected cells by 6 h. However, the injected particles did not initially carry exposed VP1SR, suggesting that they had to undergo protracted structural rearrangements before they were recognized as cargo (Vihinen-Ranta *et al*., 2000).

Although very few viral capsids are ever observed in the nuclei of infected cells (Mani *et al*., 2006; Suikkanen *et al*., 2003a), microinjection of full virions into the cytoplasm allows potential transport mechanisms to be explored. Thus, microtubule-depolymerizing drugs have been shown to block the nuclear transport of injected CPV virions, as have anti-dynein antibodies, suggesting that such free particles may be transported along microtubules. Electron micrographs of cells taken 10–12 h after infection with CPV, in which the capsids were detected by immunolabeling with nanogold particles, identified virus lying next to, and in some cases apparently associated with, the nuclear membrane, which appeared intact (Suikkanen *et al*., 2003a). However, whether these virions were associated with nuclear pores is unclear. The ~260 Å diameter of the virion means that it could, theoretically, be transported, Trojan horse-like, into nuclei via the nuclear pores, using normal cellular trafficking mechanisms, and the potential for karyopherin-mediated interactions with motifs in the VP1SR has been already been discussed at length. However, compelling evidence for such transport is lacking, and an alternate nuclear entry strategy, involving partial disruption of the nuclear membrane, has been proposed (Cohen and Pante, 2005; Cohen *et al*., 2006). These authors showed that between 1 and 4 h after infection with MVM there were dramatic changes in the shape and morphology of A9 cell nuclei, alterations in nuclear lamin immunostaining, and breaks in the nuclear envelope that increased in severity with time (Cohen *et al*., 2006). Addition of bafilomycin at hourly intervals following similar infections (Ros *et al*., 2002; S. F. C. and P. T., unpublished results) suggests that by 4-h postinfection many potentially infecting virions must still remain inside acidified vesicles, so that it will be interesting to see if damage to

the nuclear membrane becomes even more pronounced at later time points. Nevertheless, by 4 h, the lamin changes are reported to have occurred in ~20% of infected cells, although whether such changes heralded productive infection or cell death remains uncertain, and will be important to assess. Theoretically, it is difficult to envision how such mechanisms could be compatible with the subsequent unchecked entry of these damaged cells into S-phase.

Finally, both MVM and CPV infections are reported to be disrupted by various proteosome inhibitors, such as MG132, lactacystin, or epoxomicin (Ros and Kempf, 2004; Ros *et al.*, 2002), although analysis of capsid proteins during internalization in these studies showed no evidence of particle ubiquitination or degradation. Specifically, the chymotrypsin-like, but not the trypsin-like, activity of the proteosome appeared necessary, but whether this operates in the cytoplasm or nucleus, or what step in infection it might influence, remains to be determined.

However, as discussed earlier, there is a major caveat that must be considered when interpreting experiments involving drugs or other treatments that appear to interfere with parvovirus entry. Specifically, until methods are developed for directly demonstrating the arrival of the genome in the nucleus, such experiments inevitably rely on NS1 expression or the replication of viral DNA as the earliest indicator(s) of successful infection, but these events depend on the infected cell entering S-phase as part of its own replicative program. Thus, it follows that any intervention that delays or arrests the cell cycle will score as one that interferes with virus entry, whether or not it really does. Thus it is of paramount importance, for the correct interpretation of parvoviral entry experiments, to determine that the experimental approach does not itself perturb the normal cell cycle.

## E. Waiting for S-phase: Cryptic versus productive infection

Once inside the nucleus, parvoviruses must wait for the cell to enter S-phase before they can commandeer its synthetic machinery for their own preferential replication. Moreover, protracted latency occurs in parvovirus-infected animals and in noncycling cells in culture, but the location and physical state of the viral genome during this phase of the life cycle is uncertain. However, several lines of evidence suggest that it may remain sequestered within its intact particle. As discussed previously, heat-induced transitions that expose the VP1SR also expose the 3′ end of the viral DNA to polymerases, so that it is possible that the genome is ultimately extracted from the particle by the progress of the fork during complementary-strand DNA synthesis, leaving it physically attached to the capsid via interactions involving the left-end hairpin telomere. *In vitro* replicating DNA is not released from the particle until the rolling-hairpin

mechanism proceeds through a dimer intermediate, which cannot occur in the absence of the major virally coded nonstructural protein, NS1, since this mediates the necessary hairpin transitions. Thus, capsid-associated duplexes may even serve as the initial viral transcription templates, providing the NS1 necessary for their own subsequent release. Initial transcription of MVM also depends on the availability of the host transcription factor E2F, which activates its P4 promoter (Deleu *et al.*, 1999) so that viral transcription is optimized for expression during early S-phase.

While little is known of the latency strategies employed by members of the genus *Parvovirus*, AAV persistence has been explored in greater depth, and is known to involve several alternative mechanisms. In cycling human cells, but in the absence of a helper virus, genomes capable of expressing competent Rep proteins can integrate into a specific site on chromosome 13qter, although this appears to be a rare event *in vivo* (Schnepp *et al.*, 2005). Recombinant AAV (rAAV) vectors, in which genomes with viral hairpins flanking a foreign promoter-driven transgene are packaged into virions, provide additional insight into possible mechanisms of persistence in the absence of Rep expression. Because these vectors generally have identical ITRs, they give rise to virion populations with equal numbers of plus- and minus-sense genomes. When delivered *in vivo* to postmitotic cell populations at high input multiplicity, some of these genomes are able to escape from their capsids and integrate into the host genome in a site-independent manner, predominantly at the position of preexisting double-strand breaks (Miller *et al.*, 2004). More commonly, the genomes appear to emerge as unit-length episomal duplexes, perhaps by progressive annealing between complementary strands or by some sort of extensive DNA repair-driven pathway, and their ITRs then undergo intramolecular recombination, generating duplex circles (Duan *et al.*, 1998; Nakai *et al.*, 2000). These can concatamerize with time, possibly due to the recombinogenic characteristics of their ITRs, generating stable multimeric episomes. When formed *in vivo* from rAAV vector genomes, such circles can support transcription over extended periods, since they typically contain constitutive promoters and express nontoxic products.

Whether similar patterns of episomal stabilization and maintenance can occur during the life cycle of members of the *Parvovirus* genus is unknown, but seems unlikely for several reasons. First, the autonomously replicating parvoviruses almost invariably package predominantly one strand, therefore cannot give rise to duplexes in the absence of significant DNA replication. Second, each of their termini is distinct from the other, both in sequence and predicted structure, making it much less likely that they would readily undergo intramolecular recombination to form stable circular episomes. Third, the AAV2 P5 promoter drives expression of the Rep proteins, which in the absence of the helper adenovirus E1A

protein, downregulate P5, resulting in a negative feedback loop. In contrast, the parvovirus P4 promoter upregulates expression of its cytocidal product, NS1. Thus, for the parvoviruses, it appears likely that only cells arrested somewhere in the cell cycle, presumably mostly in G1, could sustain viral persistence without succumbing to the cytocidal effects of infection. This type of persistence has been termed cryptic infection (Tattersall and Gardiner, 1990) in order to distinguish it from the types of latent infection enjoyed by AAV, described above. Since infected, quiescent cell populations are difficult to maintain as such under culture conditions and cannot, by definition, be expanded, this aspect of the viral life cycle has proven difficult to explore, but it has been possible to show that autonomously replicating parvoviruses will persist in noncycling cells *in vitro*, emerging again once quiescence is broken (Paul *et al*., 1979; Tattersall, 1972). The presence of unreplicated, single-stranded DNA in the nucleus, even in quiescent cells, would be expected to strongly activate DNA damage responses through the ATM–ATR pathway, leading in normal cells to the suspension of subsequent entry into S-phase. The simplest solution to this conundrum would be for the virus to persist in the nucleus in a capsid-sequestered form, but this has yet to be explored experimentally. Once cryptically infected cells enter S-phase, however, viral DNA could be uncoated and converted to a transcriptionally competent duplex form, allowing viral gene expression to be unleashed. Since NS1 expression is concomitant with the cessation of host cell DNA synthesis, its further progress through the cell cycle must then be impeded, leaving the cell's DNA synthetic machinery at the disposal of the replicating invader.

## ACKNOWLEDGMENTS

The authors would like to acknowledge the members of our laboratory, past and present, for their contributions to many of the studies described in this chapter. We are also indebted to many collaborators and colleagues within the parvovirus research community who provided us with encouragement, preprints, and unpublished results during the gestation period of this review. The work carried out in the authors' laboratory described in this chapter was supported by USPHS Grants CA29303 and AI26109 from the National Institutes of Health.

## REFERENCES

Agbandje-Mckenna, M., and Chapman, M. S. (2006). Correlating structure with function in the viral capsid. *In* ''The Parvoviruses'' (J. Kerr, S. F. Cotmore, M. E. Bloom, R. M. Linden, and C. R. Parrish, eds.), Chap. 10, pp. 125–140. Hodder Arnold, London.

Agbandje-McKenna, M., Llamas-Saiz, A. L., Wang, F., Tattersall, P., and Rossmann, M. G. (1998). Functional implications of the structure of the murine parvovirus, minute virus of mice. *Structure* **6:**1369–1381.

Antonietti, J. P., Sahli, R., Beard, P., and Hirt, B. (1988). Characterization of the cell type-specific determinant in the genome of minute virus of mice. *J. Virol.* **62:**552–557.

Badgett, M. R., Auer, A., Carmichael, L. E., Parrish, C. R., and Bull, J. J. (2002). Evolutionary dynamics of viral attenuation. *J. Virol.* **76:**10524–10529.

Ball-Goodrich, L. J., and Tattersall, P. (1992). Two amino acid substitutions within the capsid are coordinately required for acquisition of fibrotropism by the lymphotropic strain of minute virus of mice. *J. Virol.* **66:**3415–3423.

Balsinde, J., Winstead, M. V., and Dennis, E. A. (2002). Phospholipase A2 regulation of arachidonic acid mobilization. *FEBS Lett.* **531:**2–6.

Berg, O. G., Gelb, M. H., Tsai, M. D., and Jain, M. K. (2001). Interfacial enzymology: The secreted phospholipase. *Chem. Rev.* **101:**2613–2653.

Bodendorf, U., Cziepluch, C., Jauniaux, J. C., Rommelaere, J., and Salome, N. (1999). Nuclear export factor CRM1 interacts with nonstructural proteins NS2 from parvovirus minute virus of mice. *J. Virol.* **73:**7769–7779.

Brown, W. J., Chambers, K., and Doody, A. (2003). Phospholipase A2 (PLA2) enzymes in membrane trafficking: Mediators of membrane shape and function. *Traffic* **4:**214–221.

Brownstein, D. G., Smith, A. L., Johnson, E. A., Pintel, D. J., Naeger, L. K., and Tattersall, P. (1992). The pathogenesis of infection with minute virus of mice depends on expression of the small nonstructural protein NS2 and on the genotype of the allotropic determinants VP1 and VP2. *J. Virol.* **66:**3118–3124.

Bubeck, D., Filman, D. J., Cheng, N., Steven, A. C., Hogle, J. M., and Belnap, D. M. (2005). The structure of the poliovirus 135S cell entry intermediate at 10-angstrom resolution reveals the location of an externalized polypeptide that binds to membranes. *J. Virol.* **79:**7745–7755.

Canaan, S., Zadori, Z., Ghomashchi, F., Bollinger, J., Sadilek, M., Moreau, M. E., Tijssen, P., and Gelb, M. H. (2004). Interfacial enzymology of parvovirus phospholipases A2. *J. Biol. Chem.* **279:**14502–14508.

Cater, J. E., and Pintel, D. J. (1992). The small non-structural protein NS2 of the autonomous parvovirus minute virus of mice is required for virus growth in murine cells. *J. Gen. Virol.* **73:**1839–1843.

Chandran, K., Parker, J. S., Ehrlich, M., Kirchhausen, T., and Nibert, M. L. (2003). The delta region of outer-capsid protein micro 1 undergoes conformational change and release from reovirus particles during cell entry. *J. Virol.* **77:**13361–13375.

Chang, S. F., Sgro, J. Y., and Parrish, C. R. (1992). Multiple amino acids in the capsid structure of canine parvovirus coordinately determine the canine host range and specific antigenic and hemagglutination properties. *J. Virol.* **66:**6858–6867.

Chapman, M. S., and Agbandje-McKenna, M. (2006). Atomic structure of viral particles. *In* ''The Parvoviruses'' (J. Kerr, S. F. Cotmore, M. E. Bloom, R. M. Linden, and C. R. Parrish, eds.), Chap. 9, pp. 107–124. Hodder Arnold, London.

Chapman, M. S., and Rossmann, M. G. (1993). Structure, sequence, and function correlations among parvoviruses. *Virology* **194:**491–508.

Choi, E. Y., Newman, A. E., Burger, L., and Pintel, D. (2005). Replication of minute virus of mice DNA is critically dependent on accumulated levels of NS2. *J. Virol.* **79:**12375–12381.

Clemens, K. E., and Pintel, D. J. (1988). The two transcription units of the autonomous parvovirus minute virus of mice are transcribed in a temporal order. *J. Virol.* **62:** 1448–1451.

Clinton, G. M., and Hayashi, M. (1975). The parvovirus MVM: Particles with altered structural proteins. *Virology* **66:**261–263.

Cohen, S., and Pante, N. (2005). Pushing the envelope: Microinjection of minute virus of mice into Xenopus oocytes causes damage to the nuclear envelope. *J. Gen. Virol.* **86:**3243–3252.

Cohen, S., Behzad, A. R., Carroll, J. B., and Pante, N. (2006). Parvoviral nuclear import: Bypassing the host nuclear-transport machinery. *J. Gen. Virol.* **87:**3209–3213.

Cotmore, S. F., and Tattersall, P. (1989). A genome-linked copy of the NS-1 polypeptide is located on the outside of infectious parvovirus particles. *J. Virol.* **63:**3902–3911.

Cotmore, S. F., and Tattersall, P. (1990). Alternate splicing in a parvoviral nonstructural gene links a common amino-terminal sequence to downstream domains which confer radically different localization and turnover characteristics. *Virology* **177:**477–487.

Cotmore, S. F., and Tattersall, P. (2005a). Encapsidation of minute virus of mice DNA: Aspects of the translocation mechanism revealed by the structure of partially packaged genomes. *Virology* **336:**100–112.

Cotmore, S. F., and Tattersall, P. (2005b). Genome packaging sense is controlled by the efficiency of the nick site in the right-end replication origin of parvoviruses minute virus of mice and LuIII. *J. Virol.* **79:**2287–2300.

Cotmore, S. F., and Tattersall, P. (2006a). Parvoviruses. *In* ''DNA Replication and Human Disease'' (M. L. DePamphilis, ed.), pp. 593–608. Cold Spring Harbor Laboratory Press, Cold Spring Harbor, New York.

Cotmore, S. F., and Tattersall, P. (2006b). A rolling hairpin strategy: Basic mechanisms of DNA replication in the parvoviruses. *In* ''The Parvoviruses'' (J. Kerr, S. F. Cotmore, M. E. Bloom, R. M. Linden, and C. R. Parrish, eds.), Chap. 14, pp. 5–16. Hodder Arnold, London.

Cotmore, S. F., Christensen, J., Nuesch, J. P., and Tattersall, P. (1995). The NS1 polypeptide of the murine parvovirus minute virus of mice binds to DNA sequences containing the motif (ACCA)2–3. *J. Virol.* **69:**1652–1660.

Cotmore, S. F., D'Abramo, A. M., Jr., Carbonell, L. F., Bratton, J., and Tattersall, P. (1997). The NS2 polypeptide of parvovirus MVM is required for capsid assembly in murine cells. *Virology* **231:**267–280.

Cotmore, S. F., D'Abramo, A. M., Jr., Ticknor, C. M., and Tattersall, P. (1999). Controlled conformational transitions in the MVM virion expose the VP1 N-terminus and viral genome without particle disassembly. *Virology* **254:**169–181.

D'Abramo, A. M., Jr., Ali, A. A., Wang, F., Cotmore, S. F., and Tattersall, P. (2005). Host range mutants of minute virus of Mice with a single VP2 amino acid change require additional silent mutations that regulate NS2 accumulation. *Virology* **340:**143–154.

Deleu, L., Pujol, A., Faisst, S., and Rommelaere, J. (1999). Activation of promoter P4 of the autonomous parvovirus minute virus of mice at early S phase is required for productive infection. *J. Virol.* **73:**3877–3885.

Duan, D., Sharma, P., Yang, J., Yue, Y., Dudus, L., Zhang, Y., Fisher, K. J., and Engelhardt, J. F. (1998). Circular intermediates of recombinant adeno-associated virus have defined structural characteristics responsible for long-term episomal persistence in muscle tissue. *J. Virol.* **72:**8568–8577.

Farr, G. A., and Tattersall, P. (2004). A conserved leucine that constricts the pore through the capsid fivefold cylinder plays a central role in parvoviral infection. *Virology* **323:**243–256.

Farr, G. A. (2005). The capsid five-fold cylinder and the VP1 N-terminal unique region are critical components of the parvoviral entry machine. PhD Thesis, Yale University.

Farr, G. A., Zhang, L. G., and Tattersall, P. (2005). Parvoviral virions deploy a capsid-tethered lipolytic enzyme to breach the endosomal membrane during cell entry. *Proc. Natl. Acad. Sci. USA* **102:**17148–17153.

Farr, G. A., Cotmore, S. F., and Tattersall, P. (2006). VP2 cleavage and the leucine ring at the base of the fivefold cylinder control pH-dependent externalization of both the VP1 N terminus and the genome of minute virus of mice. *J. Virol.* **80:**161–171.

Gardiner, E. M., and Tattersall, P. (1988a). Evidence that developmentally regulated control of gene expression by a parvoviral allotropic determinant is particle mediated. *J. Virol.* **62:**1713–1722.

Gardiner, E. M., and Tattersall, P. (1988b). Mapping of the fibrotropic and lymphotropic host range determinants of the parvovirus minute virus of mice. *J. Virol.* **62:**2605–2613.

Govindasamy, L., Hueffer, K., Parrish, C. R., and Agbandje-McKenna, M. (2003). Structures of host range-controlling regions of the capsids of canine and feline parvoviruses and mutants. *J. Virol.* **77:**12211–12221.

Grieger, J. C., Snowdy, S., and Samulski, R. J. (2006). Separate basic region motifs within the adeno-associated virus capsid proteins are essential for infectivity and assembly. *J. Virol.* **80:**5199–5210.

Hafenstein, S., Palermo, L. M., Kostyuchenko, V. A., Xiao, C., Morais, M. C., Nelson, C. D. S., Bowman, V. D., Battisti, A. J., Chipman, P. R., Parrish, C. R., and Rossmann, M. G. (2007). Asymmetric binding of transferrin receptor to parvovirus capsids. *Proc. Natl. Acad. Sci. USA* **104**(16)**:**6585–6589.

Heuser, J. (1989). Changes in lysosome shape and distribution correlated with changes in cytoplasmic pH. *J. Cell Biol.* **108:**855–864.

Hogle, J. M. (2002). Poliovirus cell entry: Common structural themes in viral cell entry pathways. *Annu. Rev. Microbiol.* **56:**677–702.

Horiuchi, M., Goto, H., Ishiguro, N., and Shinagawa, M. (1994). Mapping of determinants of the host range for canine cells in the genome of canine parvovirus using canine parvovirus/mink enteritis virus chimeric viruses. *J. Gen. Virol.* **75:**1319–1328.

Hueffer, K., and Parrish, C. R. (2003). Parvovirus host range, cell tropism and evolution. *Curr. Opin. Microbiol.* **6:**392–398.

Hueffer, K., Govindasamy, L., Agbandje-McKenna, M., and Parrish, C. R. (2003a). Combinations of two capsid regions controlling canine host range determine canine transferrin receptor binding by canine and feline parvoviruses. *J. Virol.* **77:**10099–10105.

Hueffer, K., Parker, J. S., Weichert, W. S., Geisel, R. E., Sgro, J. Y., and Parrish, C. R. (2003b). The natural host range shift and subsequent evolution of canine parvovirus resulted from virus-specific binding to the canine transferrin receptor. *J. Virol.* **77:**1718–1726.

Hueffer, K., Palermo, L. M., and Parrish, C. R. (2004). Parvovirus infection of cells by using variants of the feline transferrin receptor altering clathrin-mediated endocytosis, membrane domain localization, and capsid-binding domains. *J. Virol.* **78:**5601–5611.

Jongeneel, C. V., Sahli, R., McMaster, G. K., and Hirt, B. (1986). A precise map of splice junctions in the mRNAs of minute virus of mice, an autonomous parvovirus. *J. Virol.* **59:**564–573.

Kimsey, P. B., Engers, H. D., Hirt, B., and Jongeneel, C. V. (1986). Pathogenicity of fibroblast- and lymphocyte-specific variants of minute virus of mice. *J. Virol.* **59:**8–13.

Lawrence, C. M., Ray, S., Babyonyshev, M., Galluser, R., Borhani, D. W., and Harrison, S. C. (1999). Crystal structure of the ectodomain of human transferrin receptor. *Science* **286:**779–782.

Legendre, D., and Rommelaere, J. (1994). Targeting of promoters for trans activation by a carboxy-terminal domain of the NS-1 protein of the parvovirus minute virus of mice. *J. Virol.* **68:**7974–7985.

Linser, P., Bruning, H., and Armentrout, R. W. (1977). Specific binding sites for a parvovirus, minute virus of mice, on cultured mouse cells. *J. Virol.* **24:**211–221.

Llamas-Saiz, A. L., Agbandje-McKenna, M., Parker, J. S., Wahid, A. T., Parrish, C. R., and Rossmann, M. G. (1996). Structural analysis of a mutation in canine parvovirus which controls antigenicity and host range. *Virology* **225:**65–71.

Lombardo, E., Ramirez, J. C., Garcia, J., and Almendral, J. M. (2002). Complementary roles of multiple nuclear targeting signals in the capsid proteins of the parvovirus minute virus of mice during assembly and onset of infection. *J. Virol.* **76:**7049–7059.

López-Bueno, A., Mateu, M. G., and Almendral, J. M. (2003). High mutant frequency in populations of a DNA virus allows evasion from antibody therapy in an immunodeficient host. *J. Virol.* **77:**2701–2708.

López-Bueno, A., Valle, N., Gallego, J. M., Perez, J., and Almendral, J. M. (2004). Enhanced cytoplasmic sequestration of the nuclear export receptor CRM1 by NS2 mutations developed in the host regulates parvovirus fitness. *J. Virol.* **78:**10674–10684.

López-Bueno, A., Rubio, M. P., Bryant, N., McKenna, R., Agbandje-McKenna, M., and Almendral, J. M. (2006). Host-selected amino acid changes at the sialic acid binding pocket of the parvovirus capsid modulate cell binding affinity and determine virulence. *J. Virol.* **80:**1563–1573.

López-Bueno, A., Segovia, J. C., Bueren, J. A., O'Sullivan, G. M., Wang, F., Tattersall, P., and Almendral, J. M. (2007). Rapid evolution to pathogenicity of a DNA virus in an immunodeficient host targets tropism determinant residues in the capsid. (In preparation).

Mani, B., Baltzer, C., Valle, N., Almendral, J. M., Kempf, C., and Ros, C. (2006). Low pH-dependent endosomal processing of the incoming parvovirus minute virus of mice virion leads to externalization of the VP1 N-terminal sequence (N-VP1), N-VP2 cleavage, and uncoating of the full-length genome. *J. Virol.* **80:**1015–1024.

Maroto, B., Valle, N., Saffrich, R., and Almendral, J. M. (2004). Nuclear export of the non-enveloped parvovirus virion is directed by an unordered protein signal exposed on the capsid surface. *J. Virol.* **78:**10685–10694.

McMaster, G. K., Beard, P., Engers, H. D., and Hirt, B. (1981). Characterization of an immunosuppressive parvovirus related to the minute virus of mice. *J. Virol.* **38:**317–326.

Miller, D. G., Petek, L. M., and Russell, D. W. (2004). Adeno-associated virus vectors integrate at chromosome breakage sites. *Nat. Genet.* **36:**767–773.

Morais, M. C., Kanamaru, S., Badasso, M. O., Koti, J. S., Owen, B. A., McMurray, C. T., Anderson, D. L., and Rossmann, M. G. (2003). Bacteriophage phi29 scaffolding protein gp7 before and after prohead assembly. *Nat. Struct. Biol.* **10:**572–576.

Morgan, W. R., and Ward, D. C. (1986). Three splicing patterns are used to excise the small intron common to all minute virus of mice RNAs. *J. Virol.* **60:**1170–1174.

Naeger, L. K., Cater, J., and Pintel, D. J. (1990). The small nonstructural protein (NS2) of the parvovirus minute virus of mice is required for efficient DNA replication and infectious virus production in a cell-type-specific manner. *J. Virol.* **64:**6166–6175.

Nakai, H., Storm, T. A., and Kay, M. A. (2000). Recruitment of single-stranded recombinant adeno-associated virus vector genomes and intermolecular recombination are responsible for stable transduction of liver *in vivo*. *J. Virol.* **74:**9451–9463.

Nam, H. J., Gurda-Whitaker, B., Yee Gan, W., Ilaria, S., McKenna, R., Mehta, P., Alvarez, R. A., and Agbandje-McKenna, M. (2006). Identification of the sialic acid structures recognized by minute virus of mice and the role of binding affinity in virulence adaptation. *J. Biol. Chem.* **281:**25670–25677.

Palermo, L. M., Hueffer, K., and Parrish, C. R. (2003). Residues in the apical domain of the feline and canine transferrin receptors control host-specific binding and cell infection of canine and feline parvoviruses. *J. Virol.* **77:**8915–8923.

Palermo, L. M., Hafenstein, S. L., and Parrish, C. R. (2006). Purified feline and canine transferrin receptors reveal complex interactions with the capsids of canine and feline parvoviruses that correspond to their host ranges. *J. Virol.* **80:**8482–8492.

Paradiso, P. R. (1984). Identification of multiple forms of the noncapsid parvovirus protein NCVP1 in H-1 parvovirus-infected cells. *J. Virol.* **52:**82–87.

Parker, J. S. L., and Parrish, C. R. (1997). Canine parvovirus host range is determined by the specific conformation of an additional region of the capsid. *J. Virol.* **71:**9214–9222.

Parker, J. S. L., and Parrish, C. R. (2000). Cellular uptake and infection by canine parvovirus involves rapid dynamin-regulated clathrin-mediated endocytosis, followed by slower intracellular trafficking. *J. Virol.* **74:**1919–1930.

Parker, J. S. L., Murphy, W. J., Wang, D., O'Brien, S. J., and Parrish, C. R. (2001). Canine and feline parvoviruses can use human or feline transferrin receptors to bind, enter, and infect cells. *J. Virol.* **75:**3896–3902.

Parrish, C. R. (1995). Pathogenesis of feline panleukopenia virus and canine parvovirus. *Baillieres Clin. Haematol.* **8:**57–71.

Parrish, C. R., and Carmichael, L. E. (1986). Characterization and recombination mapping of an antigenic and host range mutation of canine parvovirus. *Virology* **148:**121–132.

Parrish, C. R., Aquadro, C. F., and Carmichael, L. E. (1988). Canine host range and a specific epitope map along with variant sequences in the capsid protein gene of canine parvovirus and related feline, mink, and raccoon parvoviruses. *Virology* **166:**293–307.

Parrish, C. R., Aquadro, C. F., Strassheim, M. L., Evermann, J. F., Sgro, J. Y., and Mohammed, H. O. (1991). Rapid antigenic-type replacement and DNA sequence evolution of canine parvovirus. *J. Virol.* **65:**6544–6552.

Paul, P. S., Mengeling, W. L., and Brown, T. T., Jr. (1979). Replication of porcine parvovirus in peripheral blood lymphocytes, monocytes, and peritoneal macrophages. *Infect. Immun.* **25:**1003–1007.

Pintel, D., Dadachanji, D., Astell, C. R., and Ward, D. C. (1983). The genome of minute virus of mice, an autonomous parvovirus, encodes two overlapping transcription units. *Nucleic Acids Res.* **11:**1019–1038.

Qiu, J., Yoto, Y., Tullis, G., and Pintel, D. J. (2006). Parvovirus RNA processing strategies. *In* ''The Parvoviruses'' ( J. Kerr, S. F. Cotmore, M. E. Bloom, R. M. Linden, and C. R. Parrish, eds.), Chap. 18, pp. 253–274. Hodder Arnold, London.

Riolobos, L., Reguera, J., Mateu, M. G., and Almendral, J. M. (2006). Nuclear transport of trimeric assembly intermediates exerts a morphogenetic control on the icosahedral parvovirus capsid. *J. Mol. Biol.* **357:**1026–1038.

Ros, C., and Kempf, C. (2004). The ubiquitin-proteasome machinery is essential for nuclear translocation of incoming minute virus of mice. *Virology* **324:**350–360.

Ros, C., Burckhardt, C. J., and Kempf, C. (2002). Cytoplasmic trafficking of minute virus of mice: Low-pH requirement, routing to late endosomes, and proteasome interaction. *J. Virol.* **76:**12634–12645.

Rossmann, M. G., and Palmenberg, A. C. (1988). Conservation of the putative receptor attachment site in picornaviruses. *Virology* **164:**373–382.

Rubio, M. P., López-Bueno, A., and Almendral, J. M. (2005). Virulent variants emerging in mice infected with the apathogenic prototype strain of the parvovirus minute virus of mice exhibit a capsid with low avidity for a primary receptor. *J. Virol.* **79:**11280–11290.

Schnepp, B. C., Jensen, R. L., Chen, C. L., Johnson, P. R., and Clark, K. R. (2005). Characterization of adeno-associated virus genomes isolated from human tissues. *J. Virol.* **79:**14793–14803.

Segovia, J. C., Real, A., Bueren, J. A., and Almendral, J. M. (1991). *In vitro* myelosuppressive effects of the parvovirus minute virus of mice (MVMi) on hematopoietic stem and committed progenitor cells. *Blood* **77:**980–988.

Shackelton, L. A., and Holmes, E. C. (2006). Phylogenetic evidence for the rapid evolution of human B19 erythrovirus. *J. Virol.* **80:**3666–3669.

Shackelton, L. A., Parrish, C. R., and Holmes, E. C. (2006). Evolutionary basis of codon usage and nucleotide composition bias in vertebrate DNA viruses. *J. Mol. Evol.* **62:**551–563.

Simpson, A. A., Hebert, B., Sullivan, G. M., Parrish, C. R., Zadori, Z., Tijssen, P., and Rossmann, M. G. (2002). The structure of porcine parvovirus: Comparison with related viruses. *J. Mol. Biol.* **315:**1189–1198.

Sonntag, F., Bleker, S., Leuchs, B., Fischer, R., and Kleinschmidt, J. A. (2006). Adeno-associated virus type 2 capsids with externalized VP1/VP2 trafficking domains are generated prior to passage through the cytoplasm and are maintained until uncoating occurs in the nucleus. *J. Virol.* **80:**11040–11054.

Spalholz, B. A., and Tattersall, P. (1983). Interaction of minute virus of mice with differentiated cells: Strain-dependent target cell specificity is mediated by intracellular factors. *J. Virol.* **46:**937–943.

Strassheim, M. L., Gruenberg, A., Veijalainen, P., Sgro, J. Y., and Parrish, C. R. (1994). Two dominant neutralizing antigenic determinants of canine parvovirus are found on the threefold spike of the virus capsid. *Virology* **198:**175–184.

Suikkanen, S., Saajarvi, K., Hirsimaki, J., Valilehto, O., Reunanen, H., Vihinen-Ranta, M., and Vuento, M. (2002). Role of recycling endosomes and lysosomes in dynein-dependent entry of canine parvovirus. *J. Virol.* **76:**4401–4411.

Suikkanen, S., Aaltonen, T., Nevalainen, M., Valilehto, O., Lindholm, L., Vuento, M., and Vihinen-Ranta, M. (2003a). Exploitation of microtubule cytoskeleton and dynein during parvoviral traffic toward the nucleus. *J. Virol.* **77:**10270–10279.

Suikkanen, S., Antila, M., Jaatinen, A., Vihinen-Ranta, M., and Vuento, M. (2003b). Release of canine parvovirus from endocytic vesicles. *Virology* **316:**267–280.

Tattersall, P. (1972). Replication of the parvovirus MVM I. Dependence of virus multiplication and plaque formation on cell growth. *J. Virol.* **10:**586–590.

Tattersall, P., and Bratton, J. (1983). Reciprocal productive and restrictive virus-cell interactions of immunosuppressive and prototype strains of minute virus of mice. *J. Virol.* **46:**944–955.

Tattersall, P., and Gardiner, E. M. (1990). Autonomous parvovirus-host cell interactions. *In* ''Handbook of Parvoviruses; Volume I'' (P. Tjissen, ed.), pp. 111–122. CRC Press, Boca Raton, FL.

Tattersall, P., Bergoin, M., Bloom, M. E., Brown, K. E., Linden, R. M., Muzyczka, N., Parrish, C. R., and Tijssen, P. (2005). Parvoviridae. *In* ''Virus Taxonomy, VIIIth Report of the ICTV'' (C. M. Fauquet, M. A. Mayo, J. Maniloff, U. Desselberger, and L. A. Ball, eds.), pp. 353–369. Elsevier/Academic Press, London.

Tijssen, P., Szelei, J., and Zadori, Z. (2006). Phospholipase A2 domains in structural proteins of parvoviruses. *In* ''The Parvoviruses'' (J. Kerr, S. F. Cotmore, M. E. Bloom, R. M. Linden, and C. R. Parrish, eds.), Chap. 8, pp. 95–105. Hodder Arnold, London.

Truyen, U., and Parrish, C. R. (1992). Canine and feline host ranges of canine parvovirus and feline panleukopenia virus: Distinct host cell tropisms of each virus *in vitro* and *in vivo*. *J. Virol.* **66:**5399–5408.

Truyen, U., Agbandje, M., and Parrish, C. R. (1994). Characterization of the feline host range and a specific epitope of feline panleukopenia virus. *Virology* **200:**494–503.

Truyen, U., Gruenberg, A., Chang, S. F., Obermaier, B., Veijalainen, P., and Parrish, C. R. (1995). Evolution of the feline-subgroup parvoviruses and the control of canine host range *in vivo*. *J. Virol.* **69:**4702–4710.

Tsao, J., Chapman, M. S., Agbandje, M., Keller, W., Smith, K., Wu, H., Luo, M., Smith, T. J., Rossmann, M. G., Compans, R. W., and Parrish, C. R. (1991). The three-dimensional structure of canine parvovirus and its functional implications. *Science* **251:**1456–1464.

Tullis, G. E., Burger, L. R., and Pintel, D. J. (1992). The trypsin-sensitive RVER domain in the capsid proteins of minute virus of mice is required for efficient cell binding and viral infection but not for proteolytic processing *in vivo*. *Virology* **191:**846–857.

Tullis, G. E., Burger, L. R., and Pintel, D. J. (1993). The minor capsid protein VP1 of the autonomous parvovirus minute virus of mice is dispensable for encapsidation of progeny single-stranded DNA but is required for infectivity. *J. Virol.* **67:**131–141.

Valle, N., Riolobos, L., and Almendral, J. M. (2006). Synthesis, post-translational modification and trafficking of the parvovirus structural polypeptides. *In* ''The Parvoviruses'' (J. Kerr, S. F. Cotmore, M. E. Bloom, R. M. Linden, and C. R. Parrish, eds.), Chap. 20, pp. 291–304. Hodder Arnold, London.

Vihinen-Ranta, M., and Parrish, C. R. (2006). Cell infection processes of the autonomous parvoviruses. *In* ''The Parvoviruses'' (J. Kerr, S. F. Cotmore, M. E. Bloom, R. M. Linden, and C. R. Parrish, eds.), Chap. 12, pp. 157–163. Hodder Arnold, London.

Vihinen-Ranta, M., Kakkola, L., Kalela, A., Vilja, P., and Vuento, M. (1997). Characterization of a nuclear localization signal of canine parvovirus capsid proteins. *Eur. J. Biochem.* **250:**389–394.

Vihinen-Ranta, M., Kalela, A., Makinen, P., Kakkola, L., Marjomaki, V., and Vuento, M. (1998). Intracellular route of canine parvovirus entry. *J. Virol.* **72:**802–806.

Vihinen-Ranta, M., Yuan, W., and Parrish, C. R. (2000). Cytoplasmic trafficking of the canine parvovirus capsid and its role in infection and nuclear transport. *J. Virol.* **74:**4853–4859.

Vihinen-Ranta, M., Wang, D., Weichert, W. S., and Parrish, C. R. (2002). The VP1 N-terminal sequence of canine parvovirus affects nuclear transport of capsids and efficient cell infection. *J. Virol.* **76:**1884–1891.

Vihinen-Ranta, M., Suikkanen, S., and Parrish, C. R. (2004). Pathways of cell infection by parvoviruses and adeno-associated viruses. *J. Virol.* **78:**6709–6714.

Wang, D., Yuan, W., Davis, I., and Parrish, C. R. (1998). Nonstructural protein-2 and the replication of canine parvovirus. *Virology* **240:**273–281.

Weichert, W. S., Parker, J. S., Wahid, A. T., Chang, S. F., Meier, E., and Parrish, C. R. (1998). Assaying for structural variation in the parvovirus capsid and its role in infection. *Virology* **250:**106–117.

Willwand, K., and Hirt, B. (1991). The minute virus of mice capsid specifically recognizes the 3′ hairpin structure of the viral replicative-form DNA: Mapping of the binding site by hydroxyl radical footprinting. *J. Virol.* **65:**4629–4635.

Wu, P., Xiao, W., Conlon, T., Hughes, J., Agbandje-McKenna, M., Ferkol, T., Flotte, T., and Muzyczka, N. (2000). Mutational analysis of the adeno-associated virus type 2 (AAV2) capsid gene and construction of AAV2 vectors with altered tropism. *J. Virol.* **74:**8635–8647.

Xie, Q., and Chapman, M. S. (1996). Canine parvovirus capsid structure, analysed at 2.9 Å resolution. *J. Mol. Biol.* **264:** 497–520.

Zadori, Z., Szelei, J., Lacoste, M. C., Li, Y., Gariepy, S., Raymond, P., Allaire, M., Nabi, I. R., and Tijssen, P. (2001). A viral phospholipase A2 is required for parvovirus infectivity. *Dev. Cell* **1:**291–302.